# Wind Tunnel Modeling to Determine Equivalent Building Dimensions for Alcoa Davenport Works

CPP Project 4556

January 2009

Prepared by:

Ronald L. Petersen, Principal, Ph.D., CCM
Anke Beyer-Lout, Atmospheric Scientist

**CPP, INC.**
WIND ENGINEERING AND AIR QUALITY CONSULTANTS
1415 Blue Spruce Drive
Fort Collins, Colorado 80524

Prepared for:

Alcoa
4879 State Street
Bettendorf, IA

## TABLE OF CONTENTS

## LIST OF FIGURES

## LIST OF TABLES





cpp

## LIST OF SYMBOLS

| | | |
|---|---|---|
| $AGL$ | Above Ground Level | (m) |
| $A$ | Calibration Constant | (-) |
| $B$ | Calibration Constant | (-) |
| $B_o$ | Buoyancy Ratio | (-) |
| $C$ | Concentration | (ppm or $\mu g/m^3$) |
| $C_o$ | Tracer Gas Source Strength | (ppm or $\mu g/m^3$) |
| $C_{max}$ | Maximum Measured Concentration | (ppm or $\mu g/m^3$) |
| $C_s$ | Concentration of Calibration Gas | (ppm or $\mu g/m^3$) |
| | Concentration Estimate for Full-scale Sampling Time, $t_s$ | ($\mu g/m^3$) |
| $C_k$ | Concentration Estimate for Wind tunnel Sampling Time, $t_k$ | ($\mu g/m^3$) |
| $\Delta$ | Difference Operator | (-) |
| $\Delta\theta$ | Potential Temperature Difference | (K) |
| $\delta$ | Boundary-Layer Height | (m) |
| $d$ | Stack Diameter | (m) |
| $E$ | Voltage Output | (Volts) |
| $Fr$ | Froude Number | (-) |
| $g$ | Acceleration Due to Gravity | ($m/s^2$) |
| $h$ | Stack Height Above Roof Level | (m) |
| $H$ | Stack Height Above Local Grade | (m) |
| $H_t$ | Terrain Height | (m) |
| $H_b$ | Building Height | (m) |
| $I_s$ | Gas Chromatograph Response to Calibration Gas | (Volts) |
| $I_{bg}$ | Gas Chromatograph Response to Background | (Volts) |
| $k$ | von Kármán Constant | (-) |
| $L$ | Length Scale | (m) |
| $\lambda$ | Density Ratio | (-) |
| $M_o$ | Momentum Ratio | (-) |
| $n$ | Calibration Constant, Power Law Exponent | (-) |
| $\nu$ | Kinematic Viscosity | ($m^2/s$) |
| $Q$ | Emission Rate | (g/s) |
| $\rho_a$ | Density of Ambient Air | ($kg/m^3$) |
| $\rho_s$ | Density of Stack Gas Effluent | ($kg/m^3$) |
| $R$ | Velocity Ratio | (-) |
| $R_i$ | Richardson Number | (-) |
| $Re_b$ | Building Reynolds Number | (-) |
| $Re_k$ | Roughness Reynolds Number | (-) |
| $Re_s$ | Effluent Reynolds Number | (-) |

| | | |
|---|---|---|
| $T$ | Mean Temperature | (K) |
| $t_s$ | Full-scale sampling time | (s) |
| $t_k$ | Wind tunnel sampling time | (s) |
| $U_a$ | Wind Speed at Anemometer | (m/s) |
| $U_H$ | Wind Speed at Stack Height | (m/s) |
| $U_r$ | Wind Speed at Reference Height Location | (m/s) |
| $U_\infty$ | Free Stream Wind Velocity | (m/s) |
| $U_*$ | Friction Velocity | (m/s) |
| $U$ | Mean Velocity | (m/s) |
| $U'$ | Longitudinal Root-Mean-Square Velocity | (m/s) |
| $V$ | Volume Flow Rate | ($m^3$/s) |
| $V_e$ | Exhaust Velocity | (m/s) |
| $z$ | Height Above Local Ground Level | (m) |
| $z_o$ | Surface Roughness Factor | (m) |
| $z_r$ | Reference Height | (m) |
| $z_\infty$ | Free Stream Height – 600 m above ground level | (m) |

Subscripts

| | |
|---|---|
| m | pertaining to model |
| f | pertaining to full scale |

# 1. INTRODUCTION

This report documents the wind tunnel study conducted by CPP, Inc. for for Alcoa Davenport Works (DPW) located as shown in Figures 1a and 1b. The DPW is a complex of low, large attached structures located adjacent to the Mississippi River near Davenport, IA. The plant has a length of about 1700 meters parallel to the river and 600 meters perpendicular to the river. The building heights are generally about 15-20 meters above grade. The surrounding terrain to the west rises about 30 meters above the plant elevation. There are five locations where short stacks on the facility are predicted to cause the largest contributions to the highest calculated concentration fields. These stacks are designated S-071, S-288, S-289, S-344 and S-349. The large concentration contributions are caused by building downwash using the PRIME algorithm in AERMOD. However, the building downwash algorithm within PRIME has limitations on the building aspect ratios (e.g., building width (W) divided by height (H) and building length (L) divided by height). PRIME (Schulman et al., 2000) was only tested and developed for buildings with a L/H ratio smaller than 3 and a W/H height ratio smaller than 8. For the DPW facility, the structure dimensions calculated by BPIP for input into the PRIME algorithm have much larger aspect ratios (e.g., W/H and L/H ranging from 9 to 26). Therefore, predicted concentrations using the BPIP building dimensions will have a high degree of uncertainty.

Hence, the specific purpose of this study is to determine Equivalent Building Dimensions (EBD) for AERMOD input for the above mentioned stacks. When a single solid rectangular building with the appropriate aspect ratio is adjacent or near a stack, the actual building dimensions are the appropriate model inputs. For more complicated situations, such as the DPW facility, the use of EBD for model input will result in more accurate concentration estimates for assessing compliance with the NAAQS.

At present, the only method the Environmental Protection Agency (EPA) has concurred with for determining EBD is through the use of wind tunnel modeling. Petersen, et al (1991, 1992) describes the first such study for which a protocol was reviewed and accepted by the EPA (Region V and Research Triangle Park) and for which a permit was ultimately obtained (Blewitt, 1995). That study considered the effect of a nearby lattice type (porous) structure. Also, the EPA (Tikvart, 1994) has approved the equivalent building concept, based on a study conducted by CPP (Petersen and Cochran, 1993), for regulatory modeling use on the basis that it is a source characterization study, which is under the purview of the Regional Offices. Appendix C provides a copy of a paper that was presented at the 2007 A&WMA conference that summarizes the results of an EBD study reviewed and approved by the EPA (approved in March 2007).

It should be pointed out that the EBD values determined in this study are, if anything, conservative. In general, the EBD values should be insensitive to wind speed and plume rise. There will be a point, however, where this is not true. That point occurs when the plume rise is high enough such that the plume fully escapes any effect of the building wake. At that point, all building dimension inputs are effectively zero. The Tikvart (1994) memo presents some results of stack height (i.e., plume height) sensitivity tests conducted by CPP. That study showed that the EBD values are rather insensitive to stack height (plume height) and, if anything, they tend to decrease with taller stack heights (i.e., greater plume rise). Based on the above, the wind tunnel study has been designed to simulate a low plume rise condition where the plume is most likely to be captured by building wake and eddy effects. The first conservative (low plume rise) assumption is related to the method used to simulate plume rise as discussed in detail in Section 2.2. The stack gas exit parameters used in the model underestimate plume buoyancy and hence will produce lower plume rise than actual conditions. The second conservative assumption deals with the wind speed simulated in the wind tunnel. The wind speed that is exceeded 2% of the time will be simulated for all cases and as a result low plume rise will be simulated.

This report describes the technical considerations, experimental methods, and results of the wind tunnel study designed to meet the stated project objectives.

## 2. TECHNICAL CONSIDERATIONS

### 2.1 DETERMINATION OF EQUIVALENT BUILDING DIMENSIONS

The basic modeling approach for determining equivalent building dimensions is to first document, in the wind tunnel, the dispersion characteristics as a function of wind direction at the site with all significant nearby structure wake effects included. Next, the dispersion is characterized, in the wind tunnel, with an equivalent building positioned directly upwind of the stack in place of all nearby structures (i.e., the setup as shown in Figure 2). This testing is conducted for various equivalent buildings until an equivalent building is found that provides a profile of maximum ground level concentration versus downwind distance that is similar (within the constraints defined below) to that with all site structures in place.

The criteria for defining whether or not two concentration profiles are similar is to determine the smallest building which: 1) produces an overall maximum concentration exceeding 90 percent of the overall maximum concentration observed with all site structures in place; and 2) at all other longitudinal distances, produces ground-level concentrations which exceed the ground-level concentration observed with all site structures in place less than 20 percent of the overall maximum ground-level concentration with all site structures in place. These criteria have been accepted on past EPA approved EBD studies (Petersen and Cochran, 1995a, 1995b; McBee, 1995; Thornton, 1995) and is a suggested approach in the Tikvart (1994) memorandum.

To demonstrate the method for specifying the equivalent building, consider Figure 3 which shows the maximum ground level concentration versus downwind distance for five different equivalent building setups and the maximum concentration measured with the DPW site structures in place. The figure shows that the concentration profiles for all EBDs tested meet the first criterion in that the maximum measured concentration equals at least 90 percent of the maximum concentration measured with the site structures in place. Only the case tested without an equivalent building in place (i.e. no building, just roughness) fails to meet this criterion. The 'no EB' profile also fails the second criterion at the second actual site data point (at approximately 400 m downwind) where the lower bound of the 20 percent error bar exceeds the interpolated concentration value for the 'no EB' case. The concentration profiles for all other EBDs tested meet the second criterion at all longitudinal distances. Therefore, the appropriate equivalent building for the test case shown in Figure 3 is EBD 3, since EBD 3 is the smallest equivalent building which meets both criteria.

The 20 percent error bar is based on a statistical uncertainty analysis, which has been validated from past experience which has shown that wind tunnel maximum concentrations are generally repeatable within ±10 percent (Petersen and Cochran, 1993).

## 2.2 SIMILARITY REQUIREMENTS

### 2.2.1 General

An accurate simulation of the boundary-layer winds and stack gas flow is an essential prerequisite to any wind tunnel study of diffusion from an industrial facility when *accurate* concentration estimates (i.e., ones that will compare with the real-world) are needed. The similarity requirements can be obtained from dimensional arguments derived from the equations governing fluid motion. A detailed discussion on these requirements is given in the EPA fluid modeling guideline (Snyder, 1981) and Appendix A. For EBD type studies, the criteria used for simulating plume trajectories and the ambient air flow are summarized below. These criteria maximize the accuracy of the building wake simulation and apply a conservative approach for simulating plume rise. Similar criteria have been used on past EPA approved EBD type studies (Petersen and Cochran, 1993, 1995a, 1995b, Petersen and Ratcliff, 1991, Petersen et al., 2007).

### 2.2.2 Modeling Plume Trajectories

To model plume trajectories the Momentum ratio, $M_o$, was matched in model and full scale. This quantity is defined as follows:

$$M_o = \lambda \left( \frac{V_e}{U_H} \right)^2 \qquad (1)$$

where

| | | |
|---|---|---|
| $V_e$ | = | stack gas exit velocity (m/s), |
| $U_H$ | = | ambient velocity at building top (m/s); |
| $\lambda$ | = | density ratio, $\rho_s/\rho_a$ (-). |

In addition, the stack gas flow in the model was fully turbulent upon exit as it is in the full scale. This criteria is met if the stack Reynolds number ($Re_s = dV_e/\nu_s$) is greater than 670 for buoyant plumes such as those simulated in this study (Arya and Lape, 1990). In addition, trips were installed, if required, inside the model stacks to increase the turbulence level in the exhaust stream prior to exiting the stack.

### 2.2.3 Modeling the Airflow and Dispersion

To simulate the airflow and dispersion around the buildings, the following criteria were met as recommended by EPA (1981) or Snyder (1981):

- all structures within a 732m (2266.7 ft) radius of the stacks of interest were modeled at a 1:400 scale reduction. This ensured that all structures whose critical dimension (lesser of height or width) exceeds 1/20th of the distance from the source were included in the model;
- the mean velocity profile through the entire depth of the boundary layer was represented by a power law $U/U_\infty = (z/z_\infty)^n$ where $U$ is the wind speed at height z, $U_\infty$ is the freestream velocity at $z_\infty$ and the power law exponent, n, is dependent on the surface roughness length, $z_O$, through the following equation:

$$n = 0.24 + 0.096 \log_{10} z_o + 0.016 (\log_{10} z_o)^2 \quad ; \qquad (2)$$

- Reynolds number independence was ensured: the building Reynolds number ($Re_b = U_b H_b / \nu_a$; the product of the wind speed, $U_b$, at the building height, $H_b$, times the building height divided by the viscosity of air, $\nu_a$) should be greater than 3,000 to 11,000; since the upper criteria was not met for all simulations, Reynolds number independence tests were conducted to determine the minimum acceptable operating speed for the wind tunnel;
- a neutral atmospheric boundary layer was established (Pasquill–Gifford C/D stability) by setting the bulk Richardson number ($R_{ib}$) equal to zero in model and full scale.

### 2.2.4 Summary

Using the above criteria and the source characteristics shown in Table 1, the model test conditions were computed for the stacks under evaluation. The model test conditions were computed for D stability at the 2% wind speed and are provided in the Tables included with Appendix A. Appendix A also includes a more detailed discussion on wind tunnel scaling issues.

### 2.3 EMISSION RATES

For this evaluation, emission rates are not needed. For convenience purposes, a 1 g/s emission rate were used in reporting the measured concentration results of the study. With this convention, the concentration results presented in the report can be converted to full-scale concentrations by multiplying the reported concentrations by the actual emission rates for any pollutant.

### 2.4 SURFACE ROUGHNESS

To accurately represent full scale wind profiles in the wind tunnel it is necessary to match the surface roughness length used in the model to that of the actual site. The surface roughness lengths for the DPW site were specified using AERSURFACE (EPA, 2008). For this EBD study it was necessary to define surface roughness values for the approach flow as well as for the DPW site model extents. The AERSURFACE tool with a radius of 3 km around the DPW site was used to determine the appropriate surface roughness length for the approach flow. This roughness length is more representative of the roughness upwind of the Alcoa site. To calculate the mean roughness length characteristic of the DPW facilities the AERSURFACE domain was set equal to the model extents, i.e. the area within a 732m (2266.7 ft) radius of the stacks of concern. This roughness was installed in place of the Alcoa model for the EBD test setup.

Table 2 shows the AERSURFACE results for both radii used, in 30 degree intervals around the DPW site as well as the wind tunnel test sectors. It is evident that two approach flows are necessary to accurately represent the full scale wind profiles in the wind tunnel. For wind directions of 100 through 240 degrees the surface roughness values are small with a mean of 0.084 m representing the Mississippi river to the south and east. For wind directions of 250 and 260 degrees the surface roughness value of 0.737 m is comparably high because of the industrial and suburban areas to the southwest.

The surface roughness for the Moline airport was estimated by averaging the surface roughness computed from the Moline airport AERMET meteorological data file.

### 2.5 TEST WIND SPEED

The wind speed was set at the 2% wind speed, as has been the practice on past EBD studies. The 2% wind speed for DPW was based on meteorological observations at the Moline Airport 10.0 m (32.8 ft) anemometer for the period of 2000-2004. The anemometer is located approximately 6 miles south of the DPW facilities, as shown in Figure 1a. Figure 4 shows the cumulative frequency distribution of wind speed at the Moline Airport anemometer. The wind speed distribution was used to determine the wind speed at the anemometer that is exceeded 2%

of the time (i.e., the 2% wind speed). The figure shows that the 2% wind speed is 9.0 m/s (20.1 mph) at the anemometer. All concentration tests to determine EBD were conducted with speeds at the 2% speed.

Wind speeds in the tunnel were set at a reference height of 400 m above stack grade. The speed at this reference height is determined by scaling the anemometer wind speed up to the freestream height, 600 m (Snyder, 1981) above ground level. At this height, is it assumed that wind speeds at the site and at the anemometer location are the same (i.e., local topographic effects are not important). Next, the wind speed over the site at the reference height is calculated using the wind speed at the freestream height and scaling down to the lower height using the following power law equation:

$$U_r = U_\infty \left( \frac{z_r}{z_\infty} \right)^{n_s} = U_{anem} \left( \frac{z_\infty}{z_{anem}} \right)^{n_a} \left( \frac{z_r}{z_\infty} \right)^{n_s} \qquad (3)$$

where

$U_r$ = wind speed at reference height (m/s),

$z_r$ = reference height above plant grade (400 m),

$U_\infty$ = wind speed at freestream height (m/s),

$z_\infty$ = freestream height (600 m),

$U_{anem}$ = wind speed at appropriate anemometer (m/s),

$z_{anem}$ = height above grade for $U_{anem}$ (10.0 m),

$n_a$ = wind power law exponent at the anemometer (0.15 at the Moline Airport),

$n_s$ = wind power law exponent at the site (will vary with surface roughness).

Tables A-1 through A-11 provide the calculated results using the above equations. It should be noted that the power law exponents were calculated using Equation (2) in Section 2.2 with $z_o$ equal to 0.07 m at the airport and 0.08 or 0.74 m at the DPW facilities. The surface roughness lengths for the site and the airport were specified as discussed in Section 2.4.

# 3. EXPERIMENTAL METHODS

## 3.1 Model Construction

A 1:400 scale model of for Alcoa Davenport Works and surrounding structures and terrain was constructed. The model included all significant structures (i.e., structures whose critical dimension, lesser of height or width, exceeds 1/20th of the distance from the source) within a 732 m (2266.7 ft) radius of the center of the stacks of concern at the DPW facilities. The area modeled is shown in Figures 1b and 5a. A close-up view of the modeled DPW exhaust stacks is provided in Figure 5b. The model was placed on a turntable so that different wind directions could be easily evaluated. Photographs of the model are provided in Figures 6a-d and 7a-b.

A set of solid structures, all with height to width ratios similar to those used by Huber and Snyder (1982) for development of the ISC downwash algorithm, was fabricated for placement directly upwind of each stack. These structures were used to determine the equivalent building dimensions for many building configurations. Since AERMOD is not limited to this building shape or positioning, other building shapes/positions were also investigated as appropriate to obtain the best match for the case when all site structures are present. The stacks in Table 1 and idealized buildings were tested with the turntable model removed from the wind tunnel and a uniform roughness installed in its place. The uniform roughness was constructed such that it provided approximately the same surface roughness as the test site, i.e. the area within the 732 m (2266.7 ft) radius of the center of the stacks of concern at the DPW facilities. AERSURFACE (EPA, 2008) was used to determine this surface roughness and the results can be found in Table 2.

Stacks were constructed of brass tubes and were supplied with an argon-hydrocarbon (or nitrogen-hydrocarbon) mixture of the appropriate density. A maximum of two stacks, each releasing a different hydrocarbon tracer, were operated at the same time. Measures were taken to ensure that the flow was fully turbulent upon exit. Precision gas flow meters were used to monitor and regulate the discharge velocity.

For the EBD testing, concentration sampling taps were installed on the surface of the model so that at least 46 locations were sampled simultaneously for each simulation. A typical sampling grid consists of 9 receptors located in each of 5 rows that are spaced perpendicular to the wind direction. Two background samples are located upwind of the stacks. The lateral and longitudinal spacing of receptors was designed so that the maximum concentration was defined in the lateral and longitudinal directions. A typical sampling grid is shown in Figure 8.

All testing was carried out in CPP's environmental wind tunnel shown in Figure 9. Figure 10a and b show photographs of the two configurations of the model (low roughness and high roughness approach) installed in the wind tunnel. Figures 11a and 12a depict schematics of the wind tunnel layout for these two roughness approaches with the site structures in place. For the EBD tests the site structures were removed and replaced by a uniform roughness, as discussed in Section 2.4. The wind tunnel layouts used for the EBD tests are summarized in Figures 11b and 12b for both approach roughness configurations.

Testing consisted of releasing a mixture of an inert gas and a tracer (ethane or methane) of predetermined concentration from the stacks at the required rate to simulate the desired flow rate and velocity. The flow rate of the gas mixture was controlled by a pressure regulator at the supply cylinder outlet and monitored by a precision mass flow controller. Concentration measurements were then obtained at various measurement locations. Flow straighteners and screens at the tunnel inlet were used to create a homogenous, low turbulence entrance flow. Spires and a trip downwind of the flow straighteners begin the development of the atmospheric boundary layer. The long boundary layer region between the spires and the testing location was filled with one half and two inch roughness elements, depending on the approach roughness length, placed in the repeating roughness pattern indicated in the wind tunnel as shown in Figures 11a-b and 12a-b. These roughness patterns were used to develop an approach boundary layer profile with $z_o$ = 0.08 m for the "low roughness approach" and $z_o$ = 0.74 m for the "high roughness approach".

### 3.2 Data Acquisition

Concentration, velocity, and volume flow measurements were obtained following the methods outlined in Appendix B. Atmospheric Dispersion Comparability tests were not conducted for this study as such measurements have been obtained on past studies at a similar scale.

### 3.3 Evaluation of Simulated Boundary Layer

In order to document the wind characteristics approaching the model, profiles of mean velocity and longitudinal turbulence intensity were obtained upwind of the model test area for the low roughness and high roughness configurations. The procedures for measuring the velocity profiles are provided in Appendix B. Figures 13a-b show the mean velocity and longitudinal turbulence intensity profiles that were collected directly upwind of the model turntable. To demonstrate the appropriate nature of the profiles, the target surface roughness lengths were input into the "log-law" defined as follows:

$$\frac{U}{U_*} = \frac{1}{k} \ln\left(\frac{z}{z_o}\right) \tag{4}$$

where

| | | |
|---|---|---|
| $U$ | = | velocity at height $z$, |
| $z$ | = | elevation above ground level, |
| $z_o$ | = | the surface roughness length, |
| $U_*$ | = | the friction velocity, and |
| $k$ | = | von Karman's constant (which is equal to 0.4). |

The target surface roughness lengths were 0.74 m full scale for the "high roughness approach" and 0.08 m full scale for the "low roughness approach". The left-hand plots of Figures 13a-b show that the measured and predicted velocity profiles agree well when the appropriate $z_o$ values are input into the equation.

The variation of longitudinal turbulence intensity with height has been quantified by Snyder (1981). EPA gives the following equation for predicting the variation of longitudinal turbulence intensity in the surface layer:

$$\frac{U'}{U} = n \frac{\ln\left(\frac{30}{z_o}\right)}{\ln\left(\frac{z}{z_o}\right)} \tag{5}$$

where

$$n = 0.24 + 0.096 \log_{10} z_o + 0.016 \left( \log_{10} z_o \right)^2 \tag{3}$$

and all heights are in full-scale meters. This equation is only applicable between 5 and 100 m (16 and 330 ft). Above 100 m, the turbulence intensity is assumed to decrease linearly to a value of 0.01 at a height of roughly 600 m (2000 ft) above ground level. By setting $n$ equal to 0.23 and $z_o$ to 0.74 m for the "high roughness approach" and $n$ equal to 0.16 and $z_o$ to 0.08 m for the "low roughness approach", the expected turbulence intensity profiles were estimated. The right-hand plots in Figures 13a-b show that the observed turbulence intensity profiles compare well with that estimated using Equation (5).

Concentration, velocity, and volume flow measurements were obtained following the methods outlined in Appendix B.

### 3.4 Quality Control

To ensure that accurate and reliable data are collected for assessing the plume transport and dispersion, certain quality control steps were taken. These include:

- use of blended mixtures, pure gases or certified mixtures for stack source gas;
- multipoint calibration of hydrocarbon analyzer with certified standard gas;
- calibration of stack flow measuring device with soap bubble meter;
- calibration of velocity measuring device against pitot tube; and
- wind tunnel testing to show the Reynolds number independence of the concentration measurements.

## 4. RESULTS

Concentration measurements were obtained for documenting Reynolds Number independence and determining EBD values for AERMOD input. The various tests that were conducted are described in Table 3. The normalized concentration data tabulations for each simulation are provided in Appendix D. The results for each test series are discussed below.

### 4.1 Reynolds Number Independence Tests

Tests were conducted to confirm Reynolds number independence as summarized in Table 3a. For these tests, a neutrally buoyant tracer gas was released from a 23.3 m stack (Re S_071) at the S_071 location. The measured normalized concentrations will be the same (within 10%), regardless of the Reynolds number (the wind tunnel reference speed) if Reynolds number effects are insignificant.

Ground level concentrations were evaluated for three model wind speeds (3, 4, and 5.5 m/s, set at the wind tunnel reference height of 400 m full scale). The measured concentrations were converted to full scale concentrations for a 1 g/s emission rate of any pollutant. The maximum concentrations measured at each downwind distance are shown in Figure 14. The figure also shows a line of average concentration for the 4 and 5.5 m/s model wind speeds and ±10 percent of the average for each measurement. The data sets for 4 and 5.5 m/s winds fall within the ±10 percent of the average. Some values fall outside this range at 3 m/s. Therefore, Reynolds number effects were insignificant for wind tunnel reference speeds of 4 m/s or greater and the wind tunnel tests were conducted accordingly.

### 4.2 EBD Results

Wind tunnel tests were first conducted for the wind directions of interest with all site structures in place as shown in Figure 5a. The full-scale exhaust information for the various exhausts is listed in Table 1. Five exhaust stacks with the stack identification labels: S_071, S_288, S_289, S_344, and S_349 were evaluated as shown in Figure 5b.

Ground level concentrations were measured at 45 locations for each test. The receptor grid was designed so the maximum ground level concentration versus downwind distance could be defined within acceptable uncertainty. All the stacks were evaluated for wind directions of 100 through 260 degrees at ten degree increments as shown in Table 3a. For the wind directions of 100 through 240 degrees, a "low roughness approach" surface roughness length of 0.08 m was simulated in the wind tunnel as described in Table 2 and shown in Figure 11a. For the wind directions of 250 and 260 degrees, a "high roughness approach" surface roughness length of 0.74 m was simulated in the wind tunnel as described in Table 2 and shown in Figure 12a.

For the next phase of the EBD determination for the various stacks, the site model was removed from the wind tunnel and was replaced with a uniform roughness representative of the surface roughness of the actual site (see Figures 11b and 12b). For each test, a single rectangular building was placed upwind or downwind of the stack under evaluation and the maximum ground-level concentrations versus downwind distance were measured as described above. This process was repeated for various building shapes and sizes until an EBD was found that has a similar ground level concentration profile as with all buildings present. The idealized rectangular structures (EBD structures) initially tested had height to width ratios similar to those used by Huber and Snyder (1976, 1982) for development of the ISC2 downwash algorithm (H:W:L = 1:2:1). For cases where the traditional EBD did not provide an adequate concentration profile, alternate EBD configurations were assessed. For example, wider EBD structures with the ratios of "1:4:1","1:2:2", etc. were very effective. For certain cases, the only EBD configuration that resulted in the proper profile was with the equivalent building turned at a 45 degree angle to the approach flow resulting in a corner vortex bringing the exhaust plume downward. For these cases the effective width and length ratios were calculated and used for AERMOD input. Table 3 provides a listing of building dimensions that were evaluated for each exhaust stack.

The EBD values for each wind direction were chosen using the criteria discussed in Section 2.1. The values chosen for each exhaust stack and wind direction scenario are listed in Tables 4a-e and are summarized below.

#### 4.2.1 Stack S_071 976.3' 293.3 m Pahtk 144

Table 4a shows that the largest EBD height of 22 m occurs for stack S_071 when winds are from 190 and 200 degrees. It should also be noted that when the wind come from 190 and 200 degrees as well as 110, 120, and 220 degrees, the only EBD values that matched the site profile consisted of buildings rotated so the leading edge of the structure is a corner. For these cases, corner vortices were affecting the dispersion and as a result, the rotated building configuration was the only way to obtain acceptable agreement. CPP recommends inputting a building dimensions equal to the projected width and length of the equivalent building used (see Table 4a).

No building downwash was found for wind directions of 140 degrees and 240 through 260 degrees. Therefore, no building dimension inputs are necessary for these directions.

#### 4.2.2 Stack S_288 87.2' 26.6 m 100 S Stand Hot Mill N

Table 4b shows the EBD results for stack S_288. The largest EBD height of 20 m occurs for a wind direction of 200 degrees. For most wind directions no building downwash was found for stack S_288. Therefore, no building dimension inputs are necessary for these directions.

#### 4.2.3 Stack S_289 87.2' 26.6 m 100 S Stand Hot Mill S

Table 4c shows that the largest EBD height of 20 m occurs for stack S_289 when winds come from 100 and 200 degrees. For most wind directions no building downwash was found for stack S_289. Therefore, no building dimension inputs are necessary for these directions.

#### 4.2.4 Stack S_344 84.6' 25.8 m 144 Hot Mill

Table 4d shows the EBD results for stack S_344. The largest EBD height of 22 m occurs for the wind direction of 200 degrees. EBD are only necessary for wind directions of 190 through 220 degrees. For all other wind directions no building downwash was found and no building dimension inputs are necessary.

#### 4.2.5 Stack S_349 69.9' 21.3 m

Table 4e shows that the largest EBD height of 20 m occurs for stack S_349 when winds are from 120, 130, 150, 160, 180, 190 and 210 degrees. It should also be noted that when the wind was from 100 and 110 degrees, the only EBD values that matched the site profile consisted of buildings with a height of 18 m rotated so the leading edge of the building is a corner. For these cases, corner vortices were affecting the dispersion and as a result, the rotated building configuration was the only way to obtain acceptable agreement. CPP recommends inputting a building dimensions equal to the projected width and length of the equivalent building used (see Table 4e). No building downwash was found for wind directions of 200, 220, 230, and 250 degrees. Therefore, no building dimension inputs are necessary for these directions.

### 4.3 Flow Visualization

Upon completion of the concentration testing, exhaust plume behavior was documented visually using still photographs and motion video. A dense white smoke was used to define the plume behavior.

The visualizations were conducted primarily at the wind directions and wind speeds corresponding to the worst case scenarios or scenarios of interest. The white smoke will tend to enhance the plume, thus, visually the plumes may look worse in the model than in full-scale. To properly interpret the visualizations, one should evaluate the portion of the plume that is impacting the receptor rather than the intensity of the smoke at the receptor. Photographs of selected cases are provided in Figures 16, 17 and 18. One should note that these photographs represent a snap shot in time and may not be representative of the steady-state conditions that are impacting the receptor location. The video of the flow visualization should be viewed to obtain a better qualitative understanding of plume behavior for all exhausts visualized.

When viewing the video, it should be noted that the plumes appear to be moving unrealistically fast. This apparent inconsistency is due to the fact that time is also scaled in the wind tunnel model. To estimate model time, the following equation is used:

$$t_m = t_f \left(\frac{U_f}{U_m}\right)\left(\frac{L_m}{L_f}\right) \tag{6}$$

To obtain a realistic visual picture, the video would have to be slowed down by the appropriate factor.

## 5. REFERENCES


Arya, S.P.S., and J.F. Lape, Jr., "A Comparative Study of the Different Criteria for the Physical Modeling of Buoyant Plume Rise in a Neutral Atmosphere," *Atmospheric Environment*, Vol. 24A, No. 2, pp. 289–295, 1990.

Blewitt, C., AMOCO Corporation, IL, personal communication, 1995.

EPA, "Guideline for Use of Fluid Modeling to Determine Good Engineering Practice Stack Height," USEPA Office of Air Quality, Planning and Standards, Research Triangle Park, North Carolina, EPA–450/4–81–003, July 1981.

EPA, "Guideline for Determination of Good Engineering Practice Stack Height (Technical Support Document for the Stack Height Regulation)," USEPA Office of Air Quality, Planning and Standards, Research Triangle Park, North Carolina, EPA–45014–80–023R, 1985.

EPA, "Screening Procedures for Estimating the Air Quality Impact of Stationary Sources, Revised," US EPA Office of Air and Radiation, Office of Air Quality, Planning and Standards, Research Triangle Park, North Carolina, EPA-454/R-92-019, 1992.

EPA, *User's Guide for the Industrial Source (ISC3) Dispersion Models*, EPA–454/B–95–003a, USEPA Office of Air Quality, Research Triangle Park, 1995.

EPA, *AERSURFACE User's Guide*, EPA–454/B–08–001, USEPA Office of Air Quality Planning and Standards, Air Quality Assessment Division, Air Quality Modeling Group, Research Triangle Park, North Carolina, 2008.

Greenway, A.R., J.E. Cermak, R. L. Petersen, and H.C. McCullough, "Physical Modeling Studies for GEP Stack Height Determinations," *74th Annual Meeting of the APCA*, Paper No. 81–20.3, CEP80–81 JAP–JEC33, Philadelphia, Pennsylvania, June 21–26, 1981.

Halitsky, J. A., R. L. Petersen, S.D. Taylor, and R. B. Lantz, "Nearby Terrain Effects on a Good Engineering Practice Stack Height," paper to be presented at 79th Annual APCA Meeting in Minneapolis, Minnesota, 1986.

Huber, A. H, and W. H. Snyder, "Building Wake Effects on Short Stack Effluents," *Preprint Volume for the Third Symposium on Atmospheric Diffusion and Air Quality*, American Meteorological Society, Massachusetts, 1976.

Huber, A. H., and W. H. Snyder, "Wind Tunnel Investigation of the Effects of a Rectangular-Shaped Building on Dispersion of Effluents from Short Adjacent Stacks," *Atmospheric Environment*, Vol. 16, No. 12, pp. 2837–2848, 1982.

McBee, K. L., Commonwealth of Virginia, Department of Environmental Quality, Letter to Richard D. Langford, Celco Plant, Narrows, VA, regarding acceptance of EBD study, March 15, 1995.

Petersen R. L., and M.A. Ratcliff, "Site Specific Building Height Determination for Amoco's Whiting Refinery," Report No. 90–0703, CPP, Inc., Ft. Collins, Colorado, 1991.

Petersen, R. L., D. N. Blewitt, and J. A. Panek, "Lattice Type Structure Building Height Determination for ISC Model Input," 85th Annual AWMA Conference, Kansas City, Missouri, June 21–26, 1992.

Petersen, R. L., D. K. Parce, J.L. West, and R.J. Londergan, "Effect of a Nearby Hill on Good Engineering Practice Stack Height," 86th Annual AWMA Conference, Denver, Colorado, June 13–18, 1993.

Petersen, R. L., and B. C. Cochran, "Equivalent Building Height Determinations for Cape Industries of Wilmington, North Carolina," CPP Report No. 93–0955, CPP, Inc., Ft. Collins, Colorado, 1993.

Petersen, R. L., and B. C. Cochran, "Equivalent Building Dimension Determination and Excessive Concentration Demonstration for Hoechst Celanese Corporation Celco Plant at Narrows, Virginia," CPP Report No. 93–1026, CPP, Inc., Ft. Collins, Colorado, 1995a.

Petersen, R. L., and B. C. Cochran, "Equivalent Building Dimension Determinations for District Energy St. Paul, Inc. Hans O. Nyman Energy Center, CPP Report No. 93-0979, Ft. Collins, Colorado, 1995b.

Petersen R. L., and J. Carter, "Evaluation of AERMOD/PRIME For Two Sites with Unusual Structures," 99th Annual AWMA Conference, New Orleans, Louisiana, June 20-23, 2006.

Petersen, R. L., J. Reifschneider, D. Shea, D. Cramer, and L. Labrie, "Improved Building Dimension Inputs for AERMOD Modeling of the Mirant Potomac River Generating Station," 100th Annual A&WMA Conference, Pittsburgh, PA, June 2007.

Schulman, L. L., D. G. Strimaitis, and J. S. Scire, "Development and Evaluation of the PRIME Plume Rise and Building Downwash Model," *J. Air & Waste Manage. Assoc.*, Vol. 50, pp. 378-390, 2000.

Snyder, W. H., "Guideline for Fluid Modeling of Atmospheric Diffusion," USEPA, Environmental Sciences Research Laboratory, Office of Research and Development, Research Triangle Park, North Carolina, Report No. EPA600/8–81–009, 1981.

Thornton, J. D., Section Manager, Air Quality Division, Minnesota Pollution Control Agency, Letter Approving EBD study for District Energy St. Paul, April 4, 1995.

Tikvart, J.A. , Chief, Source Receptor Analysis Branch, United States Environmental Protection Agency, Letter to Brenda Johnson, Regional Modeling Contact, Region IV and Douglas Neeley, Chief Air Programs Branch, Region IV, July 25, 1994.

Turner, D.B., "Workbook of Atmospheric Dispersion Estimates," Lewis Publishers, Boca Raton, Florida, 33431, 1994

# FIGURES


Figure 1. Site maps: a) site location and project anemometer

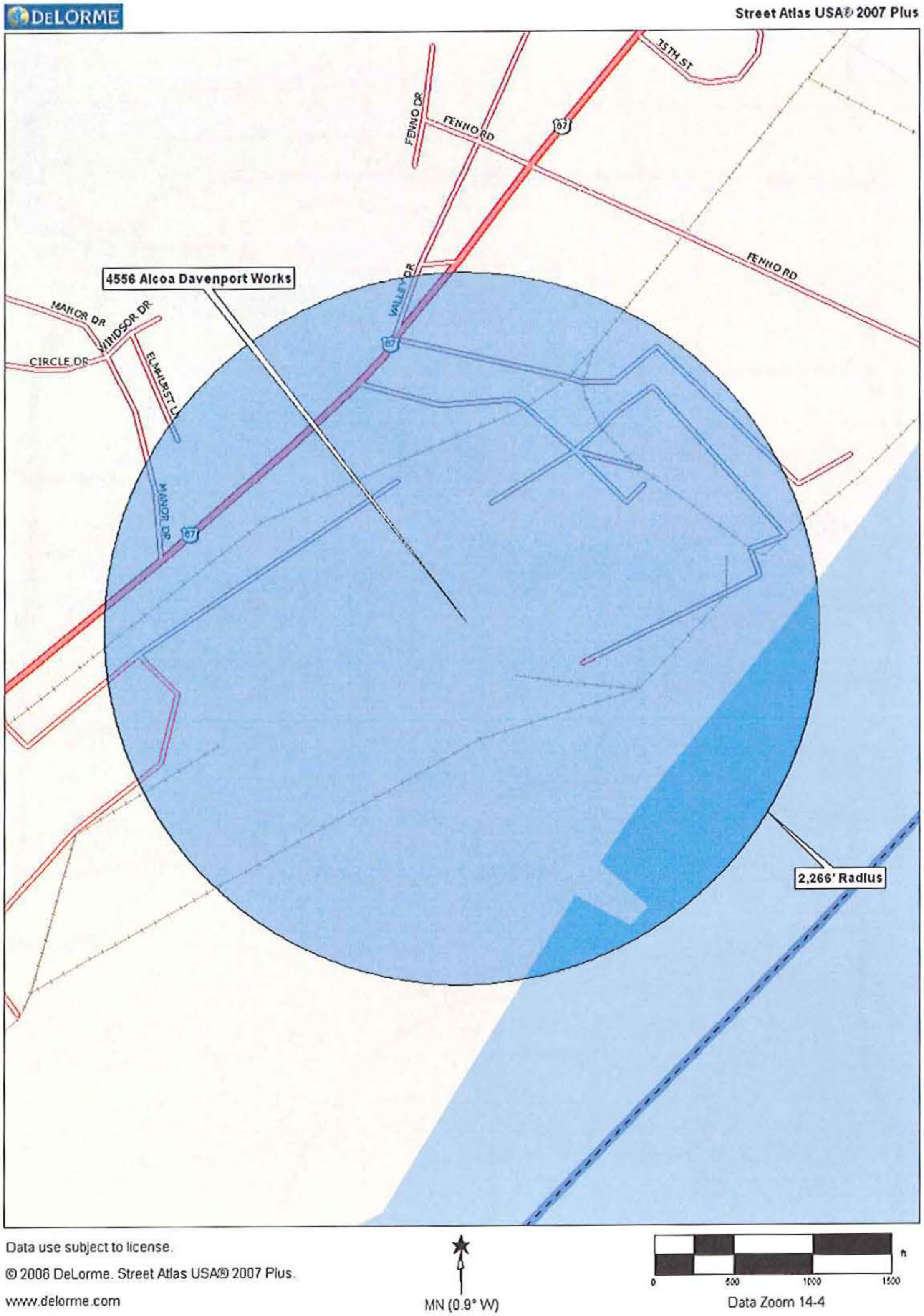


Figure 1. Site maps: b) extents of model turntable.

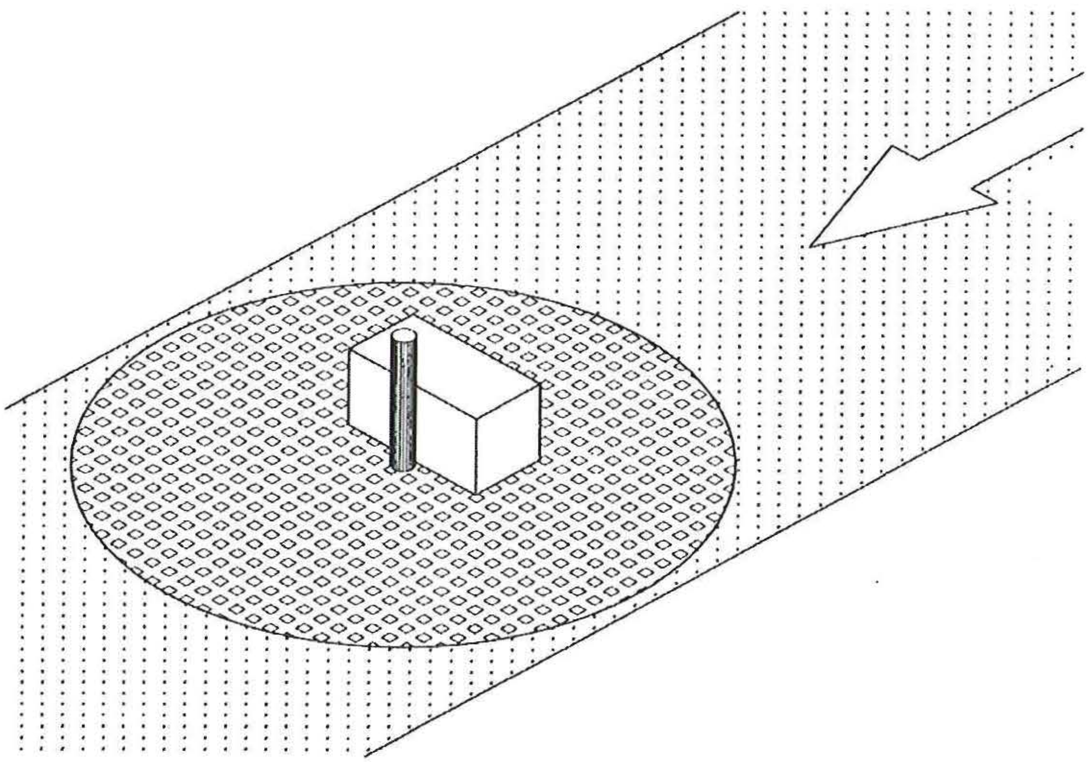

Figure 2. AERMOD idealized building and stack configuration and EBD wind tunnel setup.

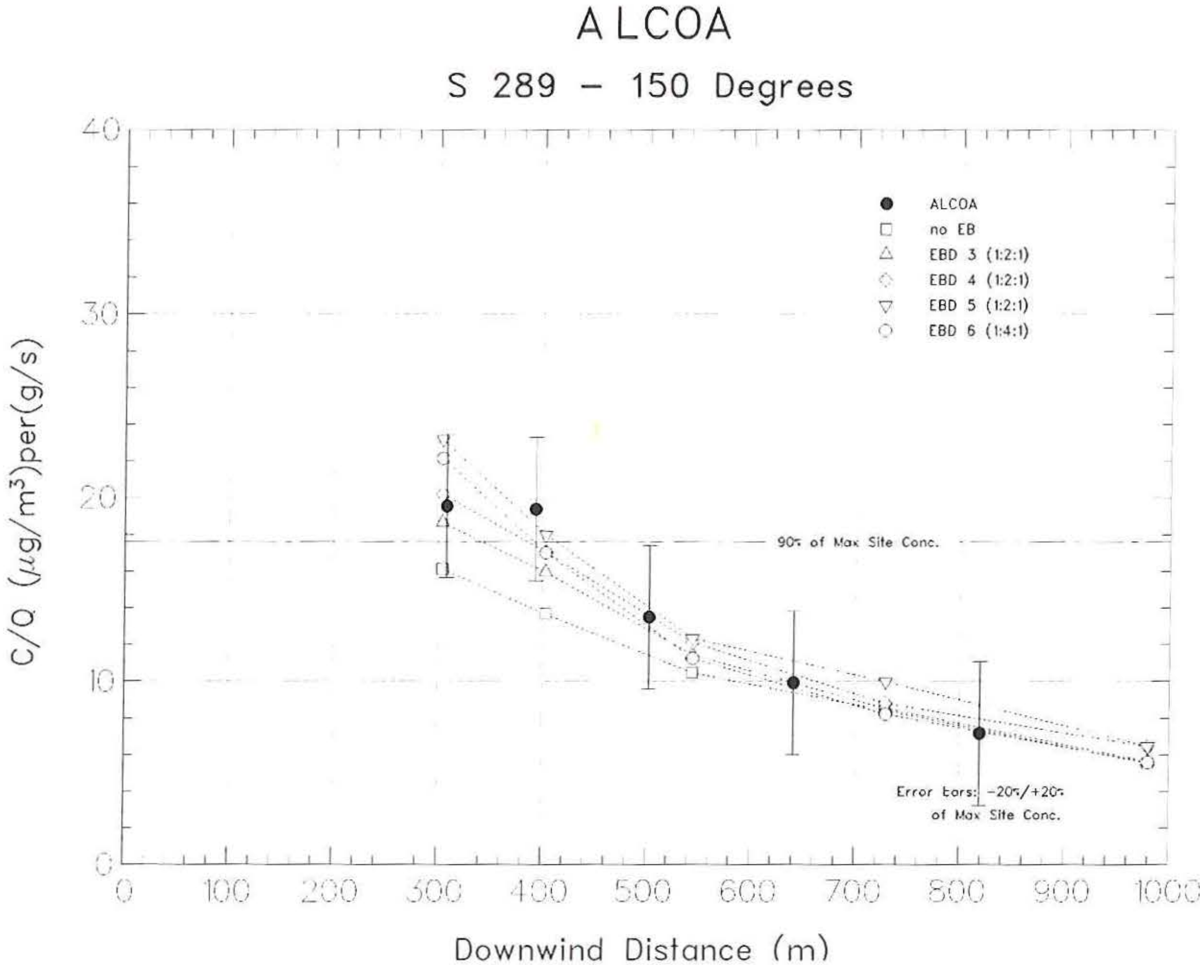


Figure 3. Typical results from the DPW equivalent building determination study. The figure shows the maximum concentration versus downwind distance with 20 percent error bar with the site structures in place, a horizontal line at 0.9 times the maximum concentration with site structures in place, and maximum concentration values versus distance for various equivalent buildings.

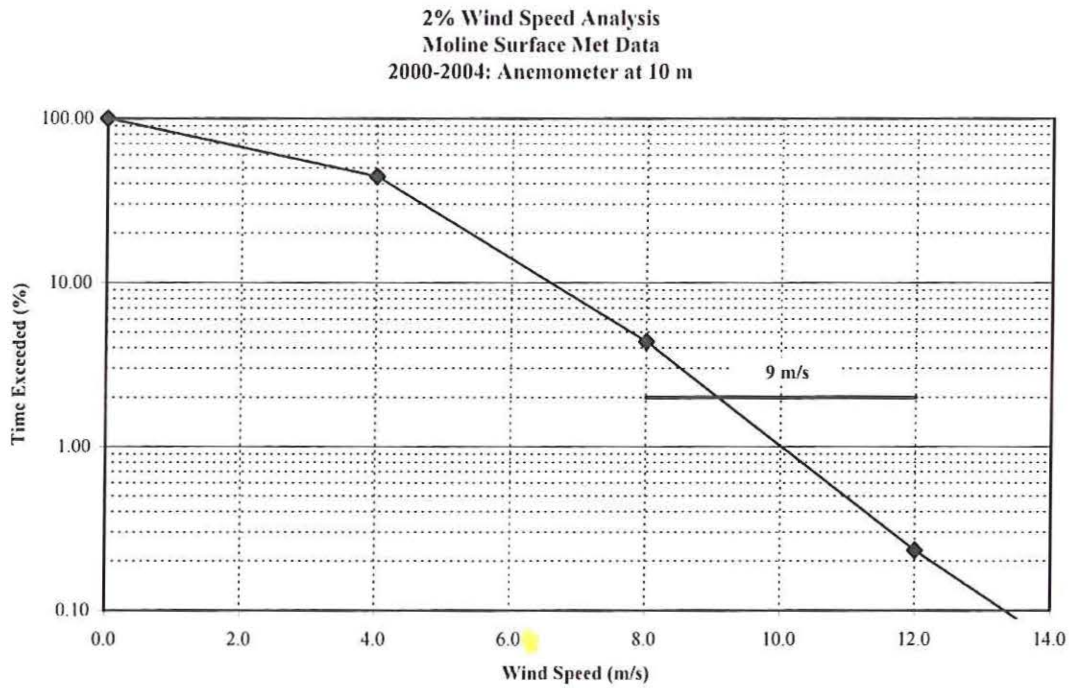


**Joint Probability Distribution of Wind Speed and Wind Direction at the Moline Surface Met Data Anemometer**

| Category: / Maximum Wind Speed (m/s): | 1 / 4.0 | 2 / 8.0 | 3 / 12.0 | 4 / 16.0 | 5 / >16 | Totals by Direction (%) |
|---|---|---|---|---|---|---|
| N | 2.008 | 1.646 | 0.078 | 0.000 | 0.000 | **3.7** |
| NNE | 2.301 | 1.630 | 0.039 | 0.000 | 0.000 | **4.0** |
| NE | 2.063 | 1.376 | 0.058 | 0.000 | 0.000 | **3.5** |
| ENE | 2.492 | 2.079 | 0.169 | 0.002 | 0.000 | **4.7** |
| E | 3.821 | 2.648 | 0.207 | 0.004 | 0.000 | **6.7** |
| ESE | 5.048 | 1.945 | 0.165 | 0.008 | 0.000 | **7.2** |
| SE | 3.115 | 1.410 | 0.079 | 0.002 | 0.000 | **4.6** |
| SSE | 2.463 | 2.006 | 0.175 | 0.003 | 0.000 | **4.6** |
| S | 3.209 | 3.495 | 0.497 | 0.015 | 0.000 | **7.2** |
| SSW | 3.198 | 4.374 | 0.688 | 0.025 | 0.000 | **8.3** |
| SW | 3.672 | 3.520 | 0.491 | 0.047 | 0.010 | **7.7** |
| WSW | 5.063 | 2.690 | 0.365 | 0.048 | 0.009 | **8.2** |
| W | 4.891 | 3.000 | 0.399 | 0.051 | 0.000 | **8.3** |
| WNW | 3.479 | 3.518 | 0.308 | 0.001 | 0.000 | **7.3** |
| NW | 2.280 | 3.134 | 0.325 | 0.009 | 0.000 | **5.7** |
| NNW | 1.317 | 1.537 | 0.104 | 0.000 | 0.000 | **3.0** |
| Calm | 5.200 | | | | | |
| **Totals by Category (%):** | **55.6** | **40.0** | **4.1** | **0.2** | **0.0** | **100** |

Figure 4. Percent time indicated wind speed is exceeded at the Moline Airport anemometer.

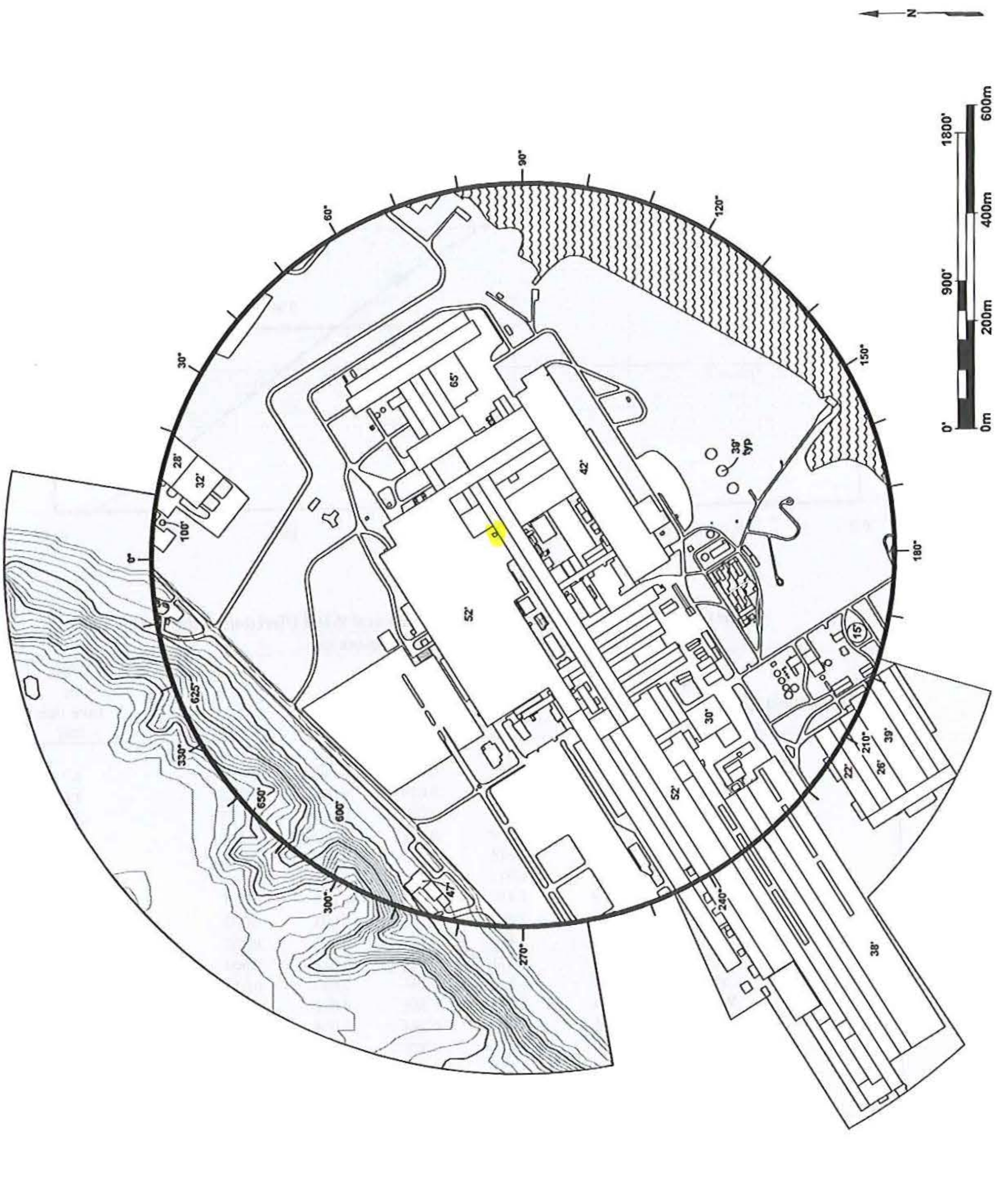


Figure 5. Plan view of: a) the area modeled with building heights.

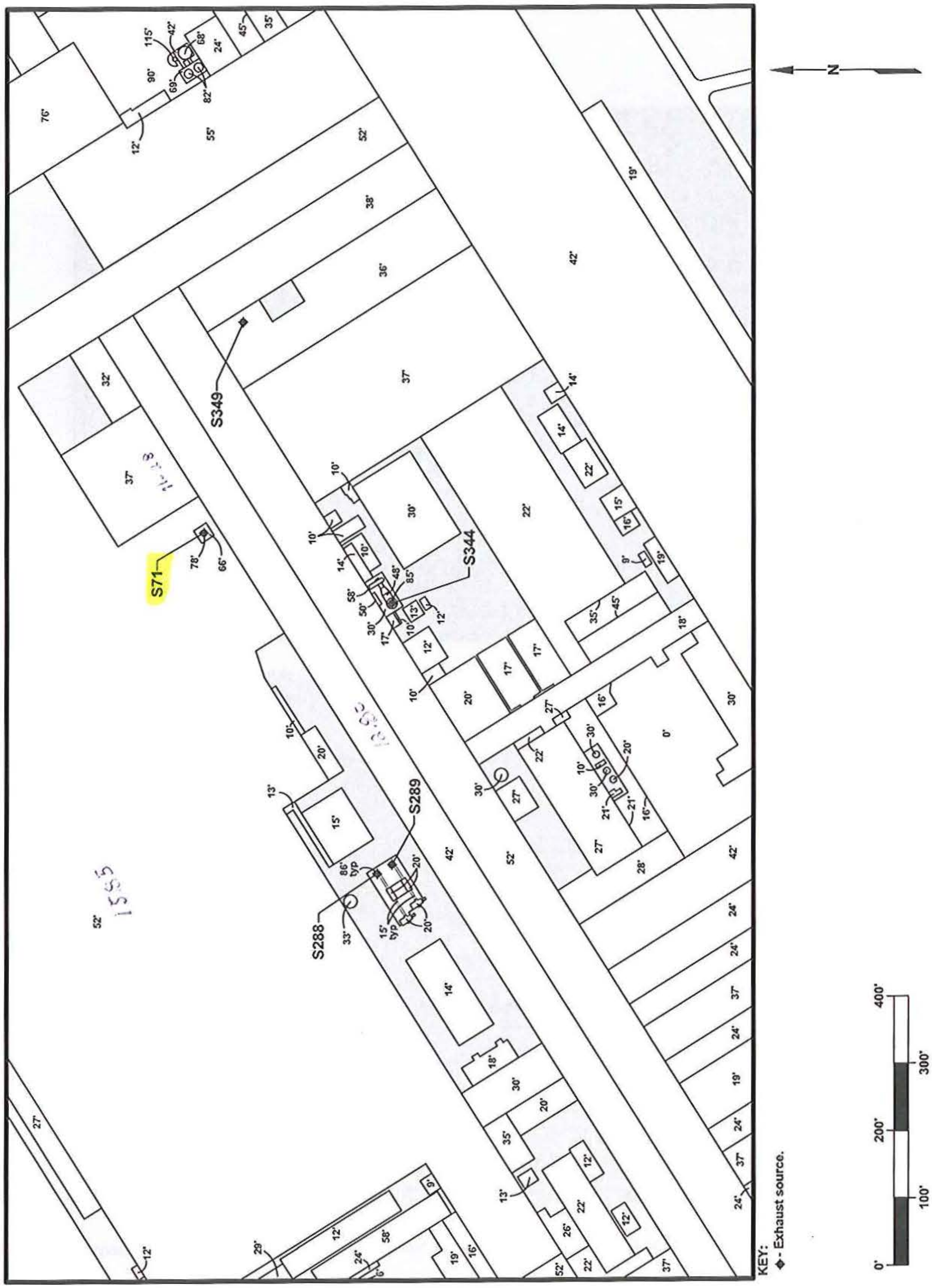


Figure 5. Plan view of: b) the DPW facility with tier heights and source locations.

a)

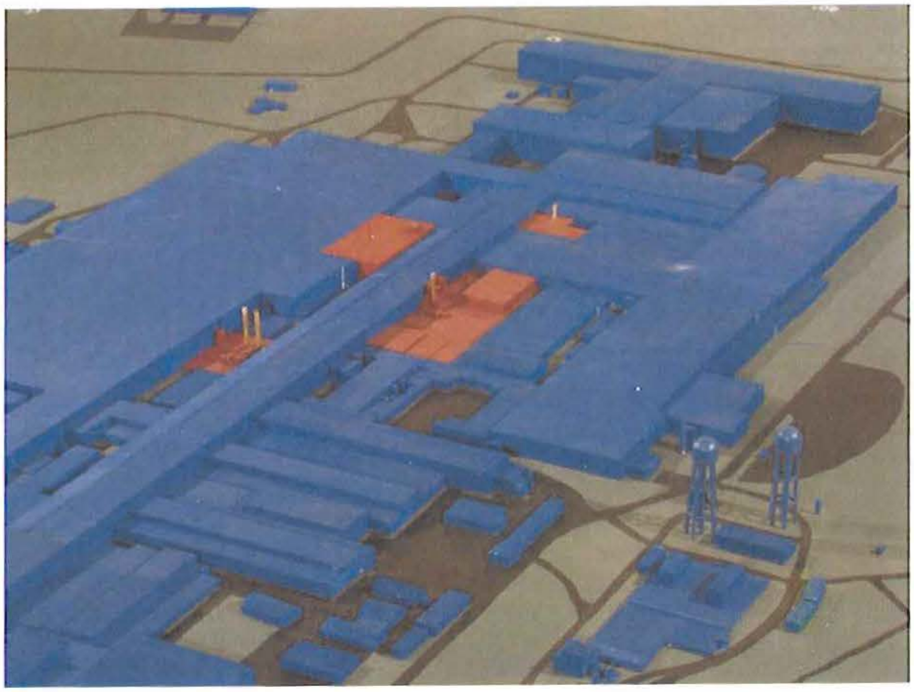

b)

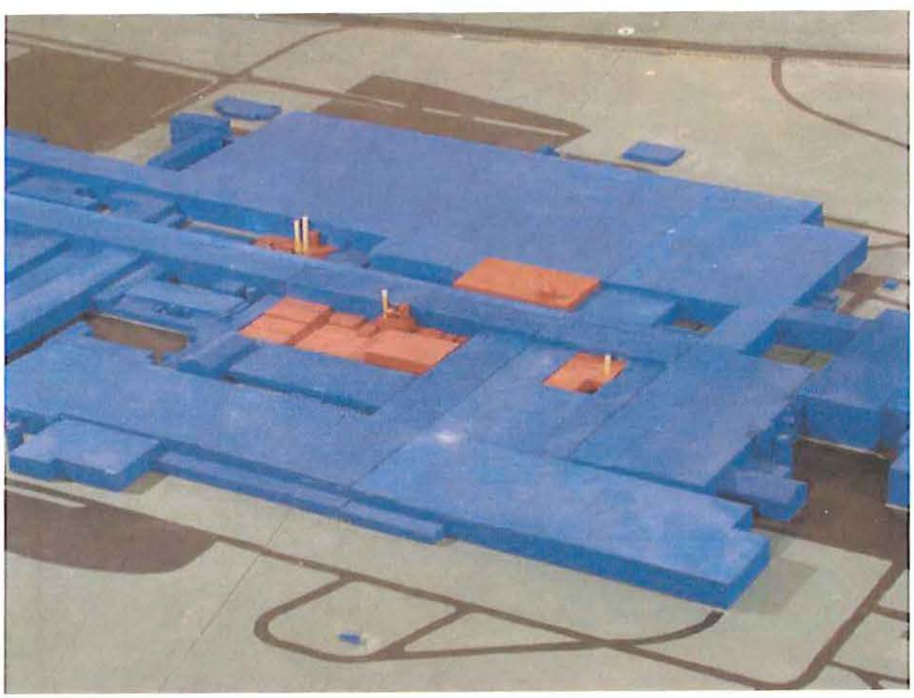

Figure 6. Photographs of the model looking from: a) the southwest; b) the southeast.

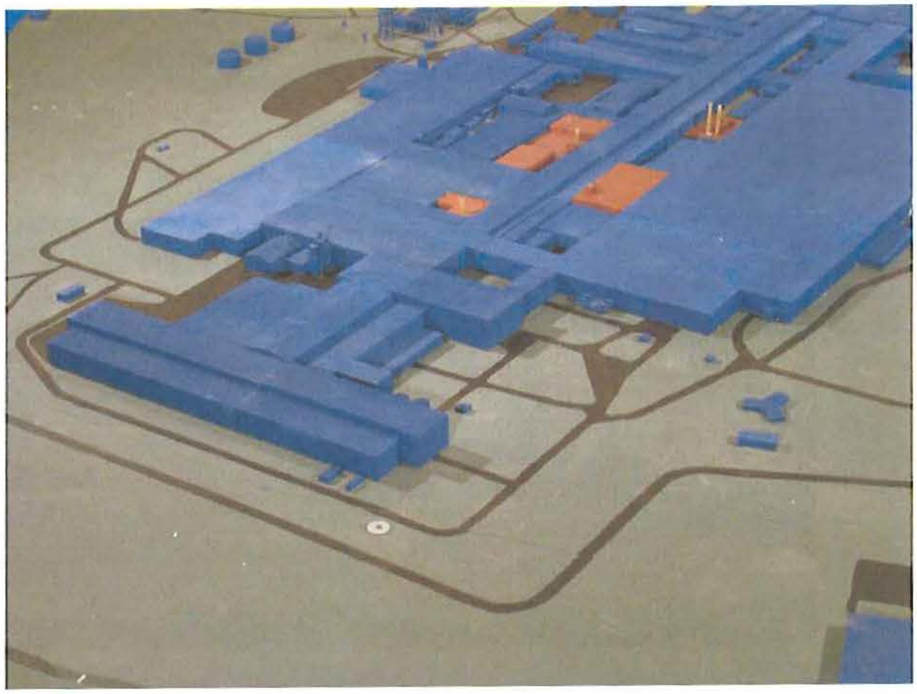

c)

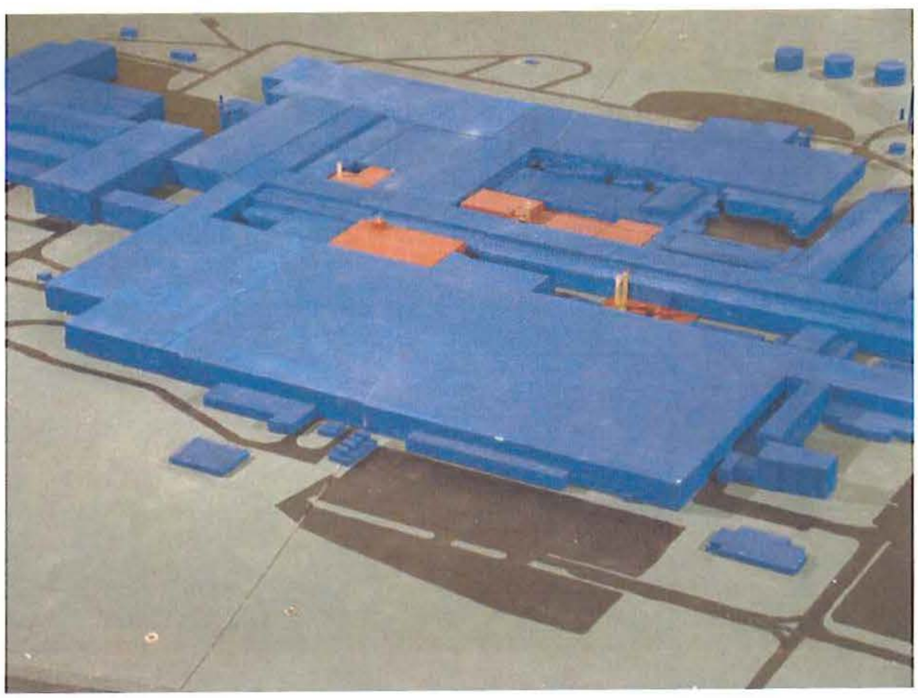

d)

Figure 6. Photographs of the model looking from: c) the northeast; d) the northwest.

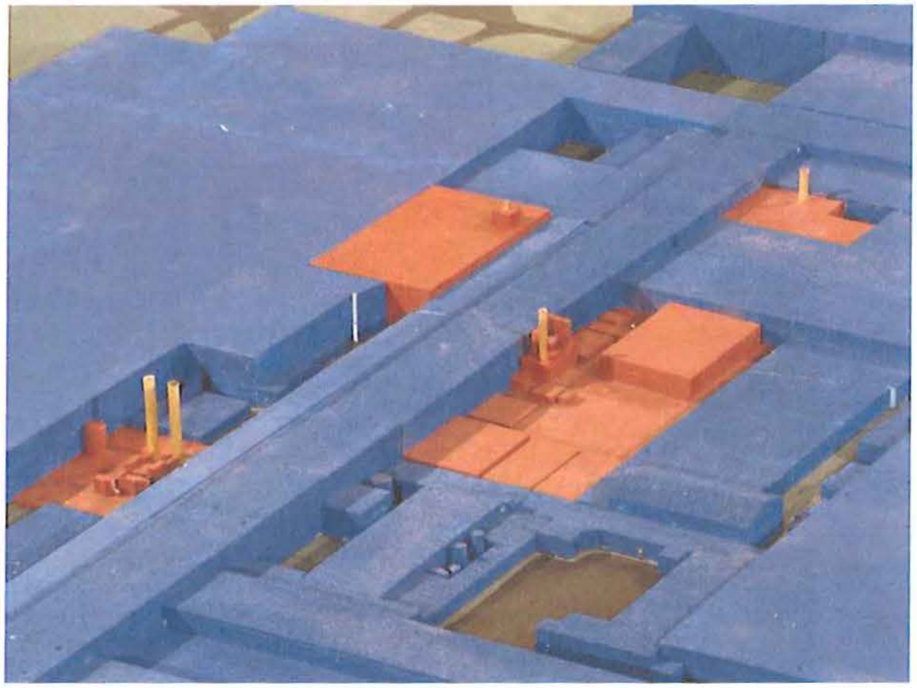

a)

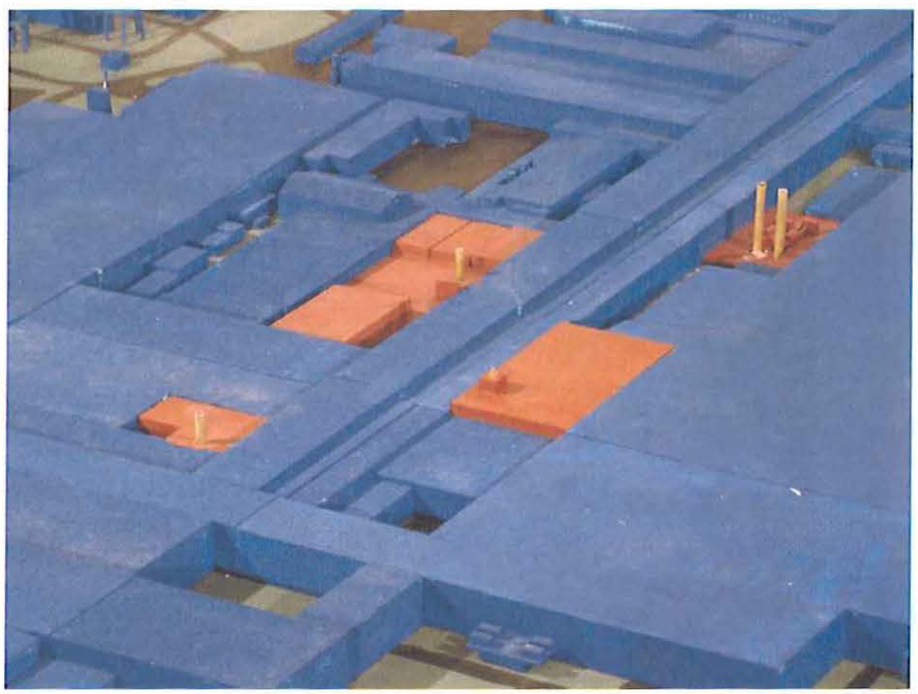

b)

Figure 7. Close-up photographs of the model looking from: a) the southwest; b) the northeast.

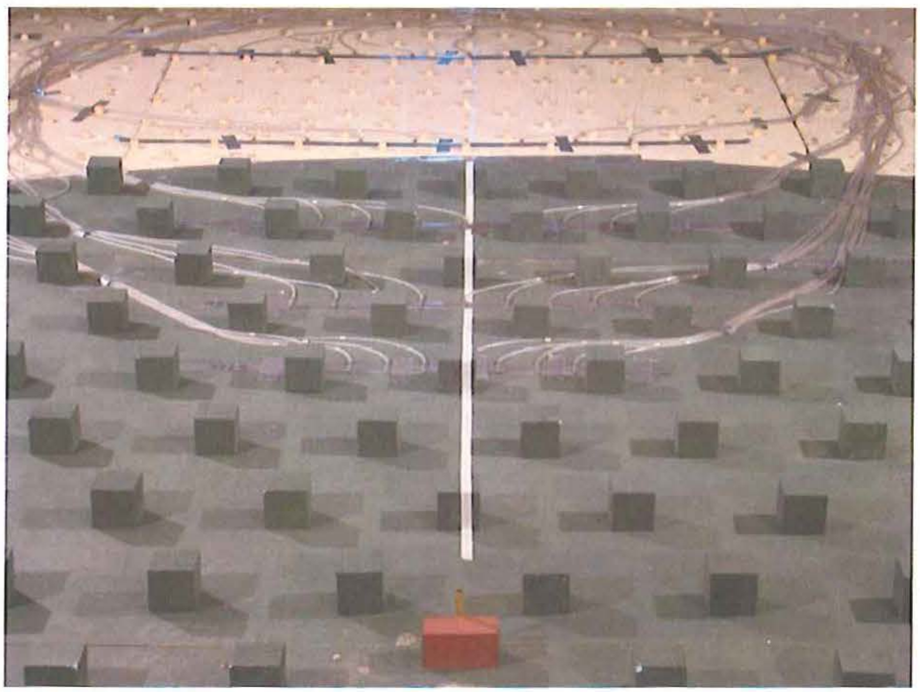

Figure 8. Typical ground-level concentration sampling grid.

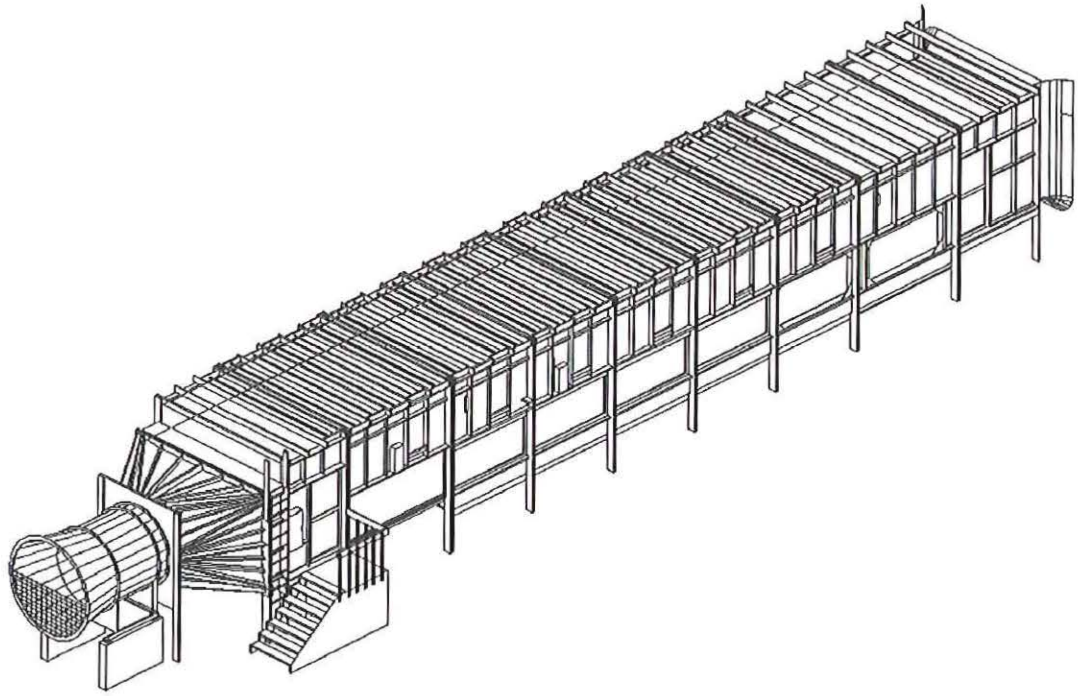

**CPP's Open-Circuit Wind Tunnel Performance Specifications**

| | | |
|---|---|---|
| 1. | **Dimensions** | |
| | *Test Section Length* | *74.5 ft (22.7m)* |
| | *Test Section Width* | *12 ft (3.7m)* |
| | *Ceiling Height* | *Variable from 5.5 ft to 8.5 ft (1.7 m to 2.6 m)* |
| 2. | **Wind tunnel Fan** | |
| | *Horse Power* | *20 hp (15 kW)* |
| | *Drive Type* | *8 blade axial fan, two-speed motor* |
| | *Speed Control* | *Coarse: 900/600 rpm, 2 speed motor*<br>*Fine: blade pitch control* |
| 3. | **Temperature** | |
| | *Ambient Air* | *Not Controlled* |
| | *Test Section Surface* | *-50 °F to 120 °F (-46 °C to 49 °C)* |
| 4. | **Boundary-Layer** | |
| | *Free Stream Velocities* | *0.0 fps to 30.0 fps (0.0 to 9.1 m/s)* |
| | *Boundary-Layer Thickness* | *Up to 6.0 ft (1.8 m)* |
| 5. | **Stream wise Pressure Gradient** | *Zeroed by ceiling adjustment* |

Figure 9. CPP's open-circuit wind tunnel used for testing.

a)

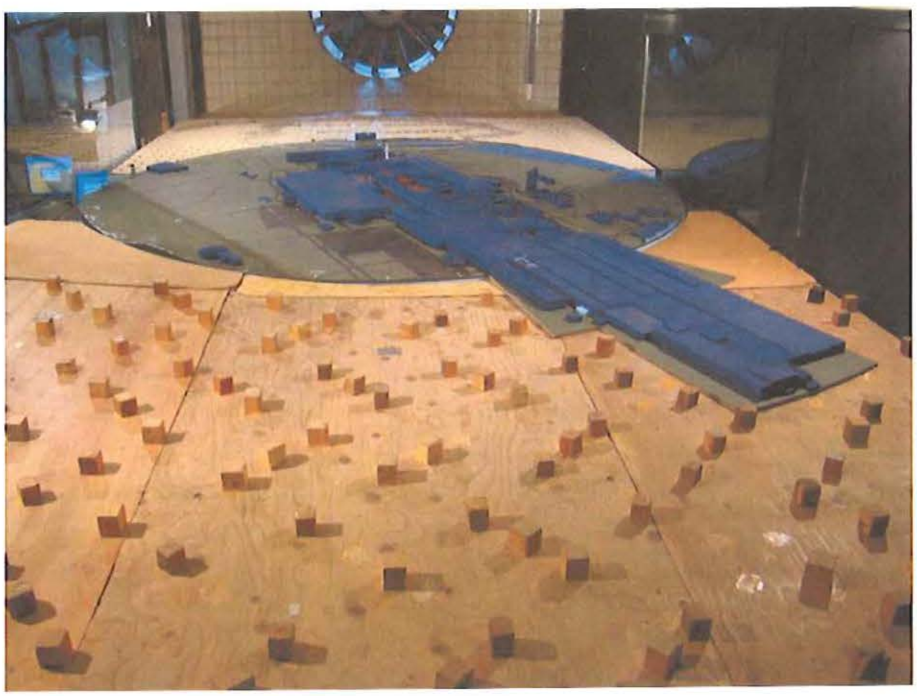

b)

Figure 10. Photographs of the wind tunnel configurations: a) low roughness approach ($z_o$ = 0.08 m); b) high roughness approach ($z_o$ = 0.74 m).

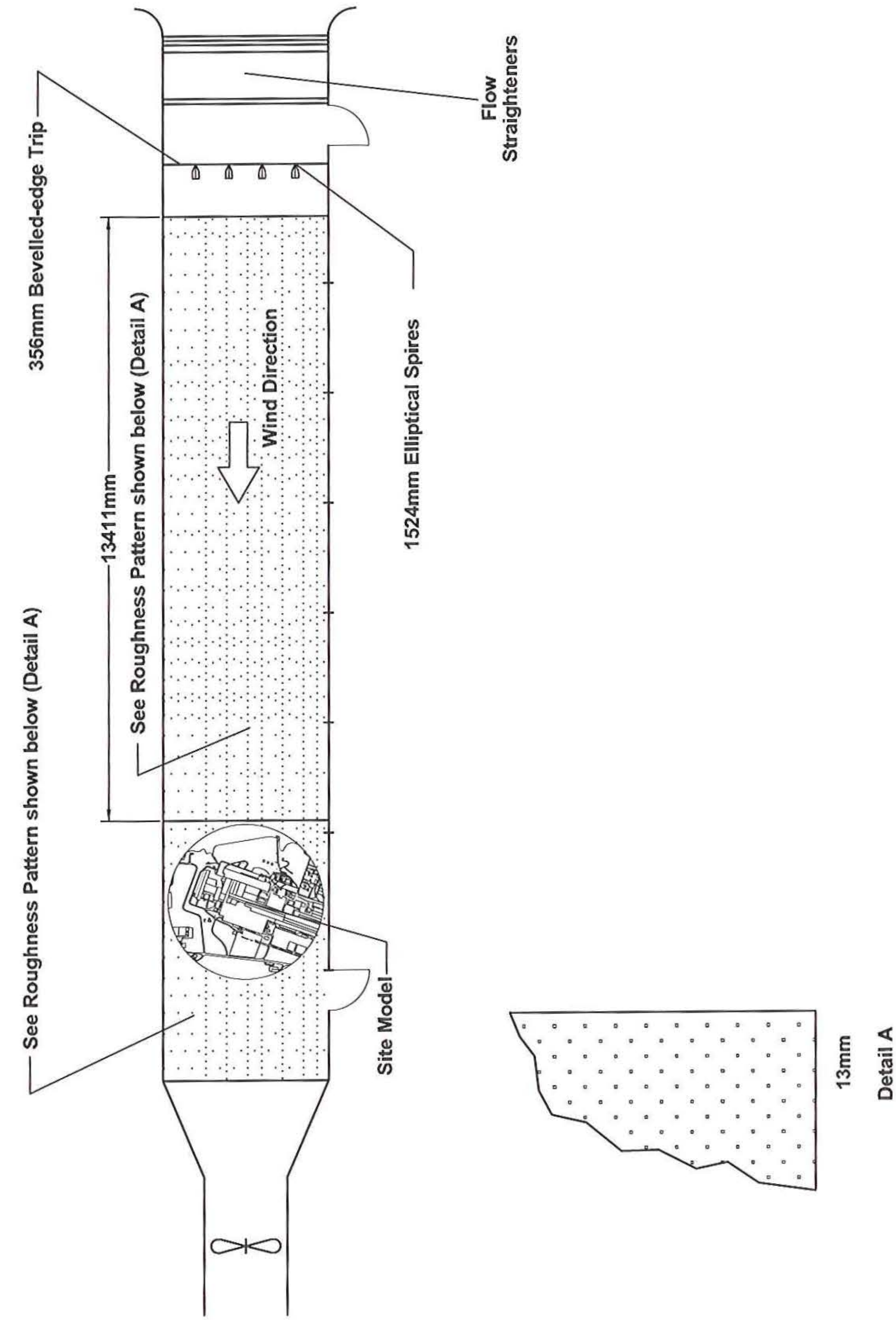


Figure 11. Low roughness approach wind tunnel setup for: a) tests with all site structures in place.

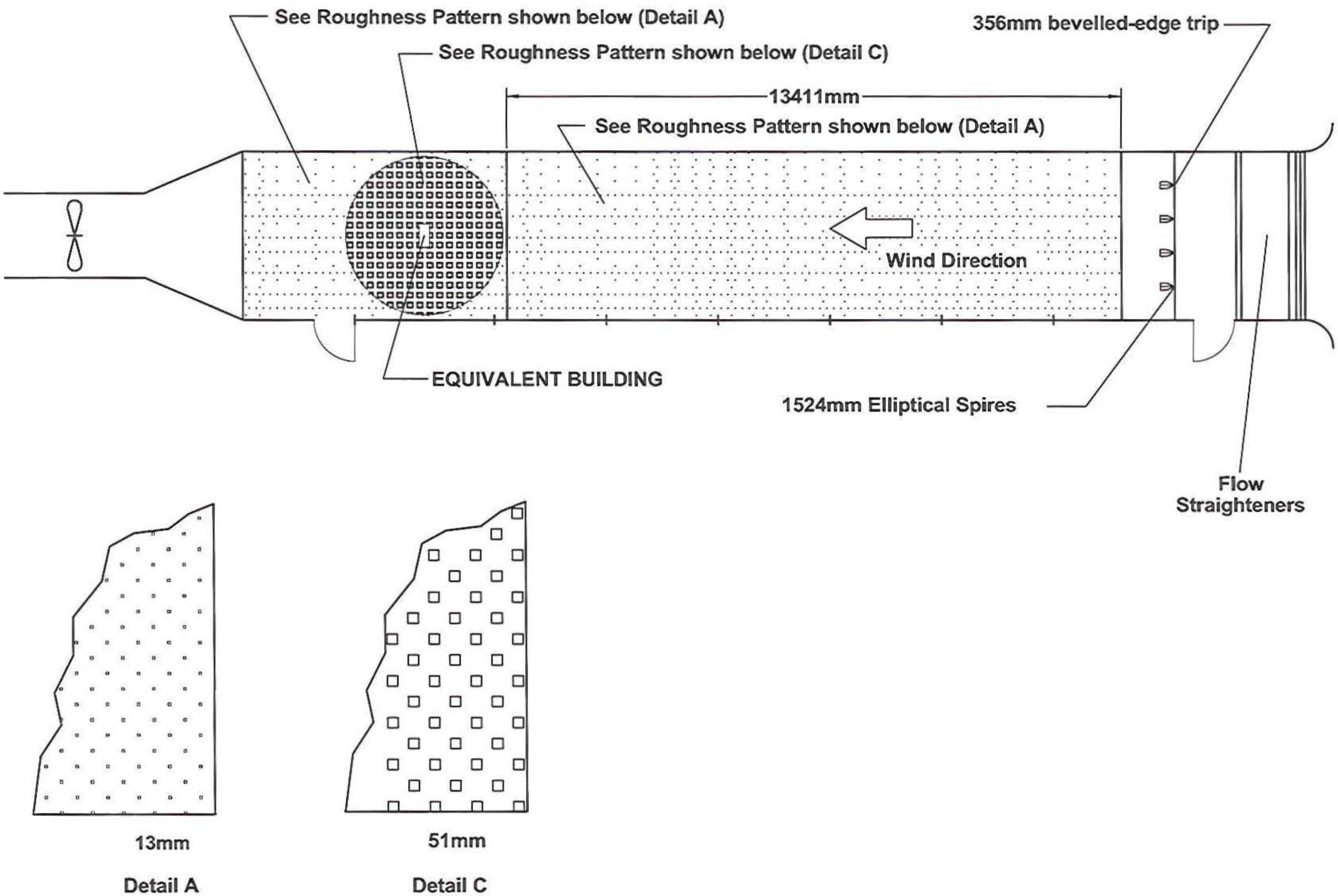


Figure 11. Low roughness approach wind tunnel setup for: b) EBD tests with uniform roughness in place.

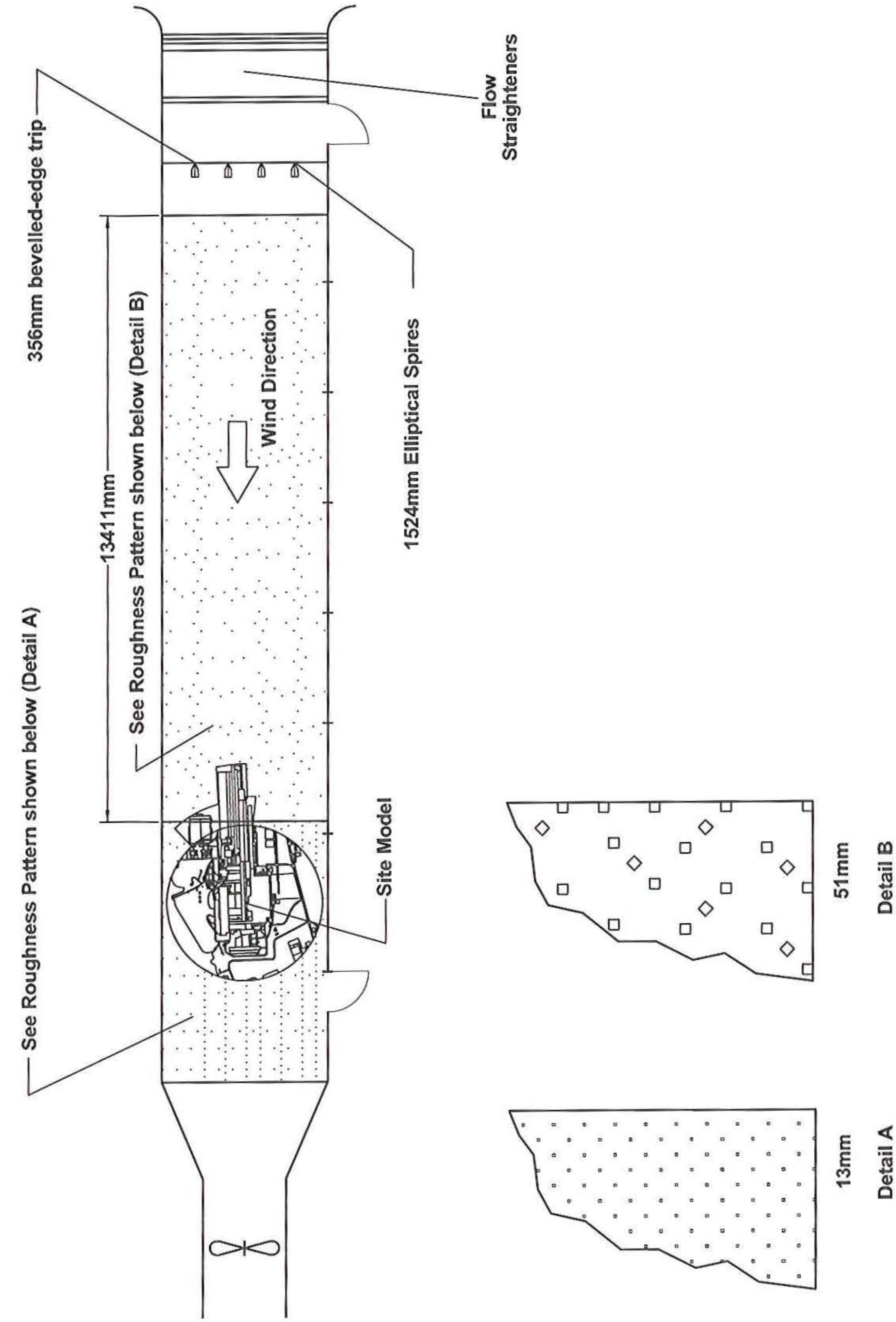


Figure 12. High roughness approach wind tunnel setup for: a) tests with all site structures in place.

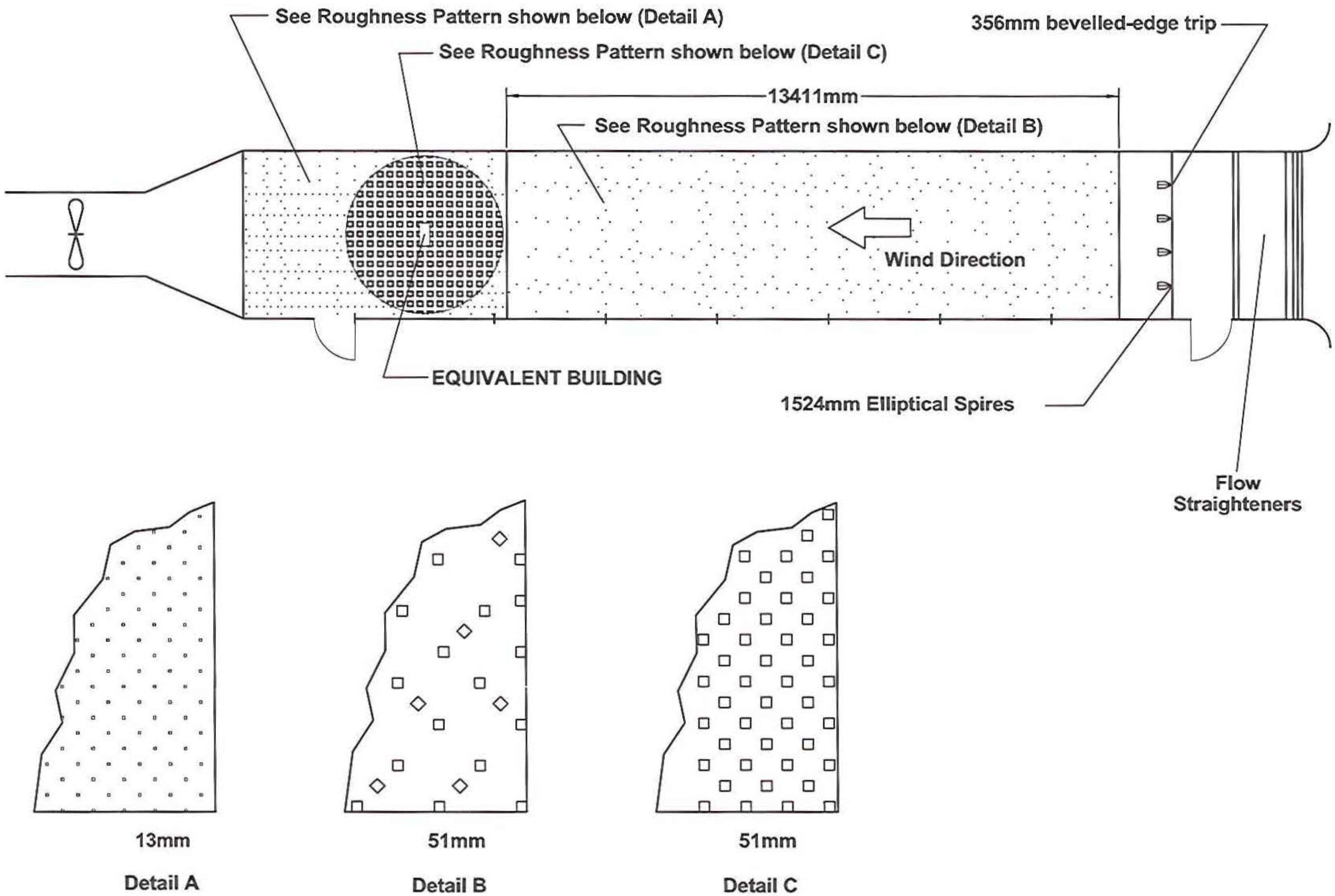


Figure 12. High roughness approach wind tunnel setup for: b) EBD tests with uniform roughness in place.

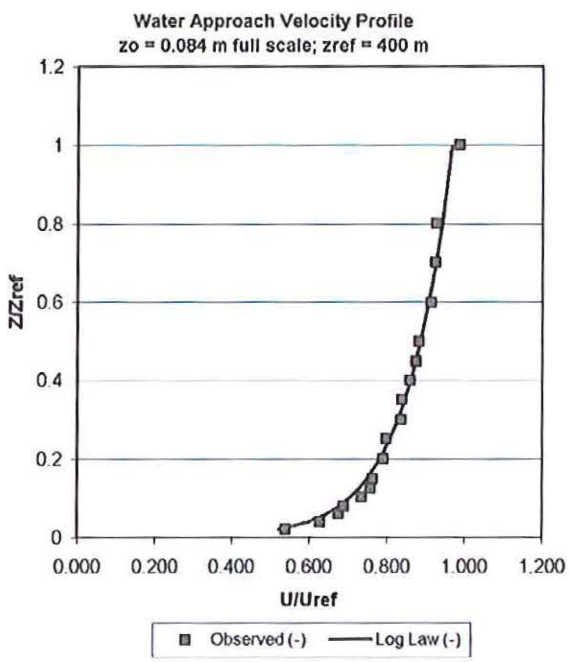


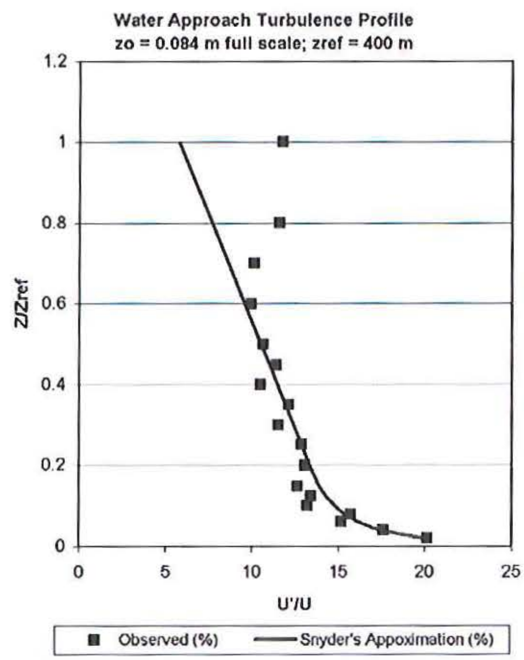


Figure 13. Mean longitudinal velocity and turbulence intensity profiles approaching model for: a) low roughness approach.

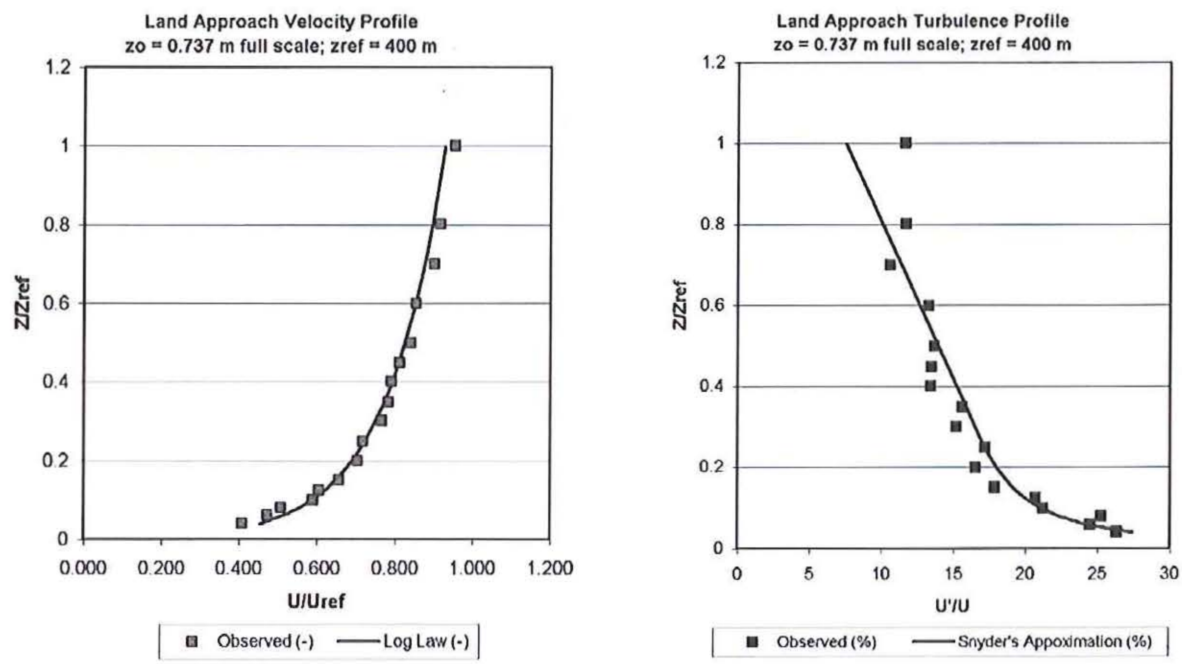


Figure 13. Mean longitudinal velocity and turbulence intensity profiles approaching model for: b) high roughness approach.

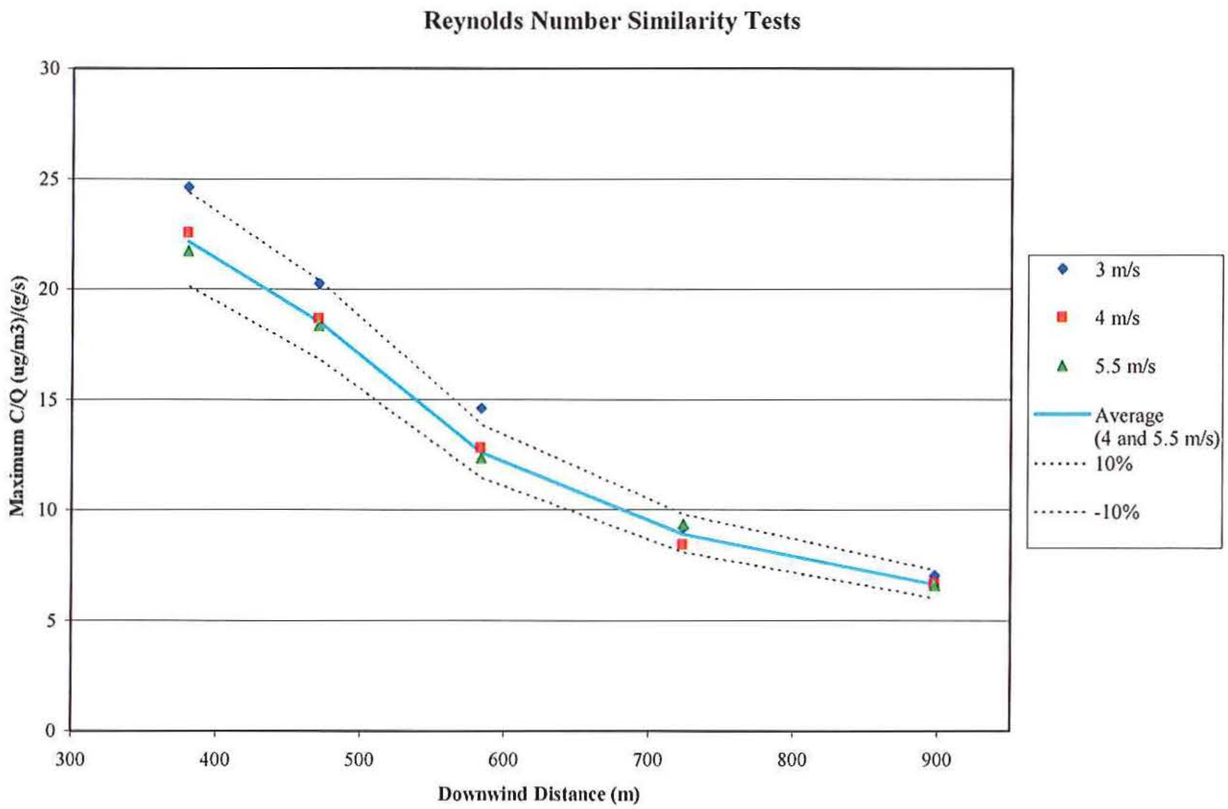


Figure 14. Maximum C/Q (µg/m³)/(g/s) versus distance for various wind tunnel speeds – demonstrates Reynolds number independence.

a)

b)

Figure 15. Photographs of selected exhaust plume flow visualizations for stack S_289: a) site structures in place for a wind direction of 100 degrees; b) site structures in place for a wind direction of 140 degrees.

c)

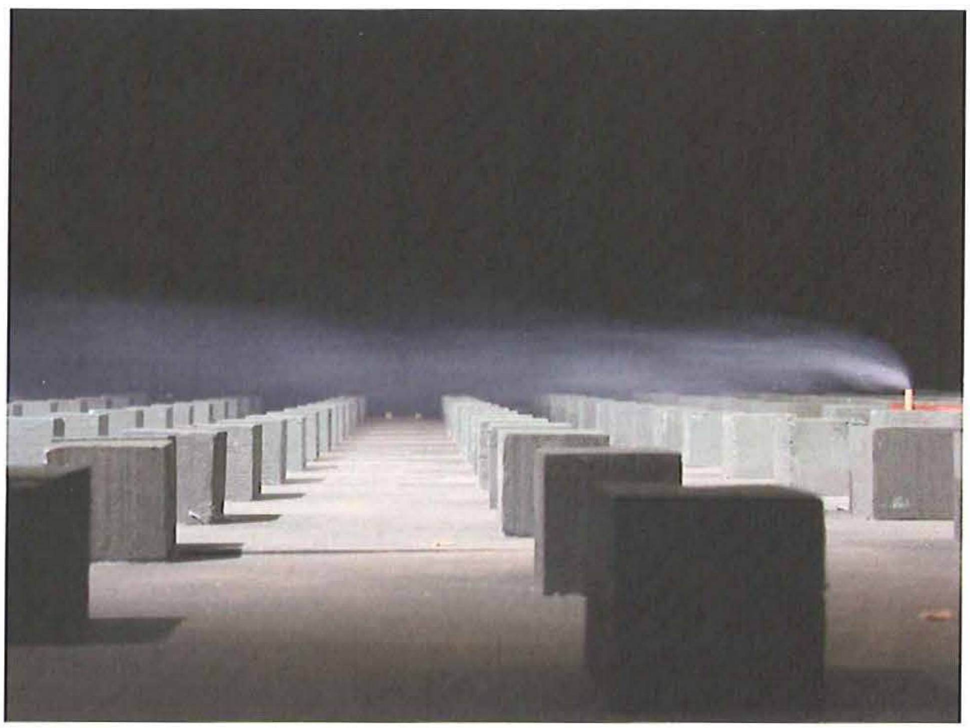

d)

Figure 15. Photographs of selected exhaust plume flow visualizations for stack S_289: c) EBD tests: no building in place; d) EBD tests: EBD 6 (1:4:1) with a full scale height of 24 m in place.

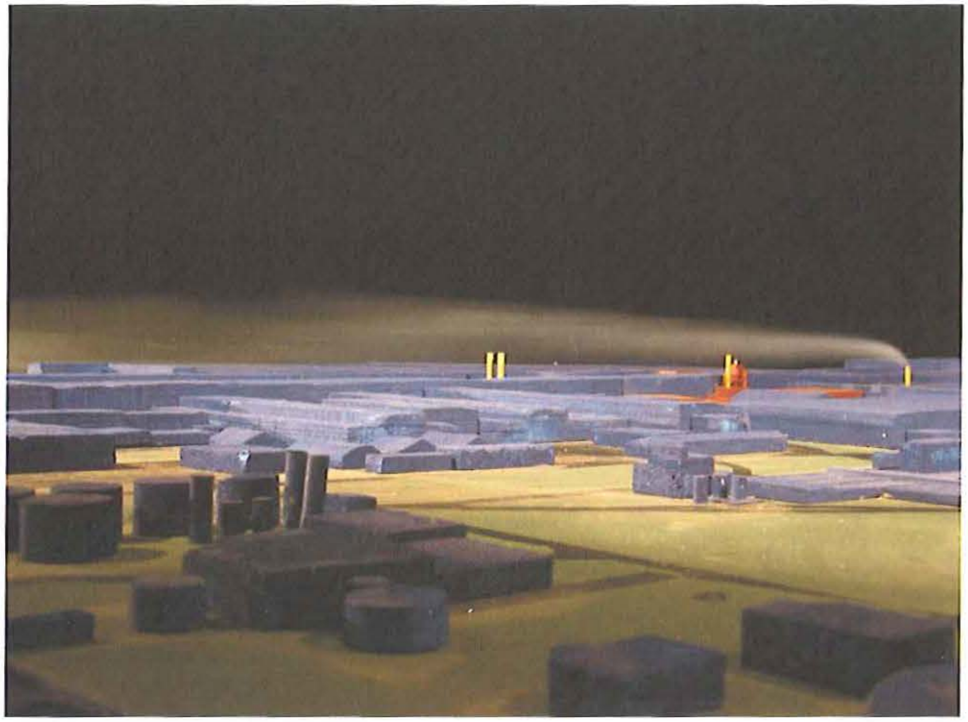

a)

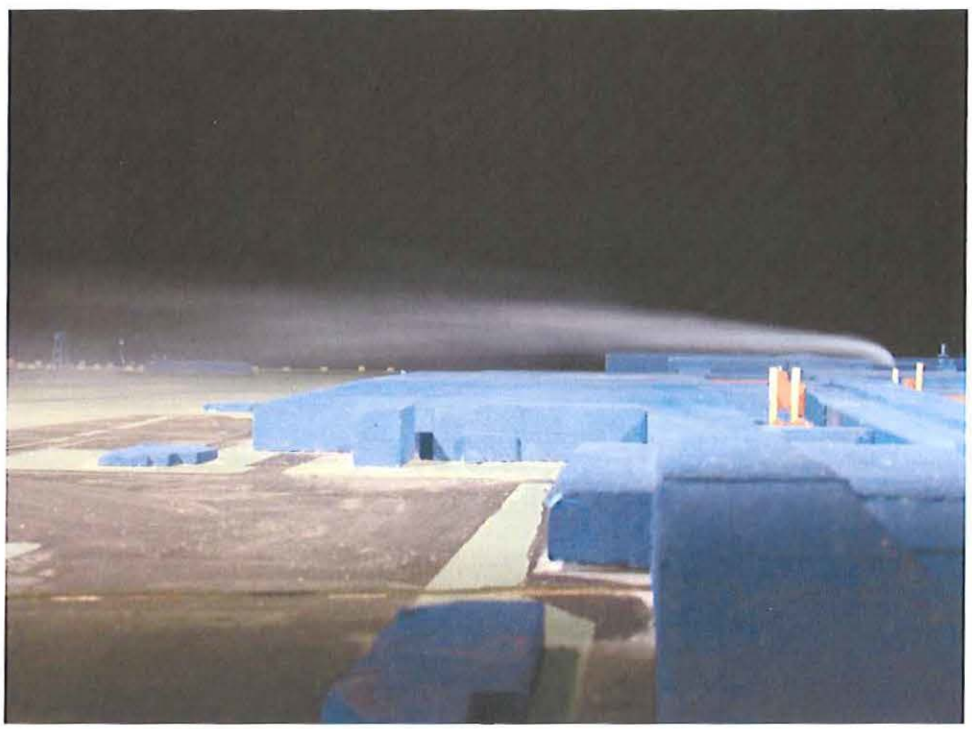

b)

Figure 16. Photographs of selected exhaust plume flow visualizations for stack S_349: a) site structures in place for a wind direction of 100 degrees; b) site structures in place for a wind direction of 140 degrees.

c)

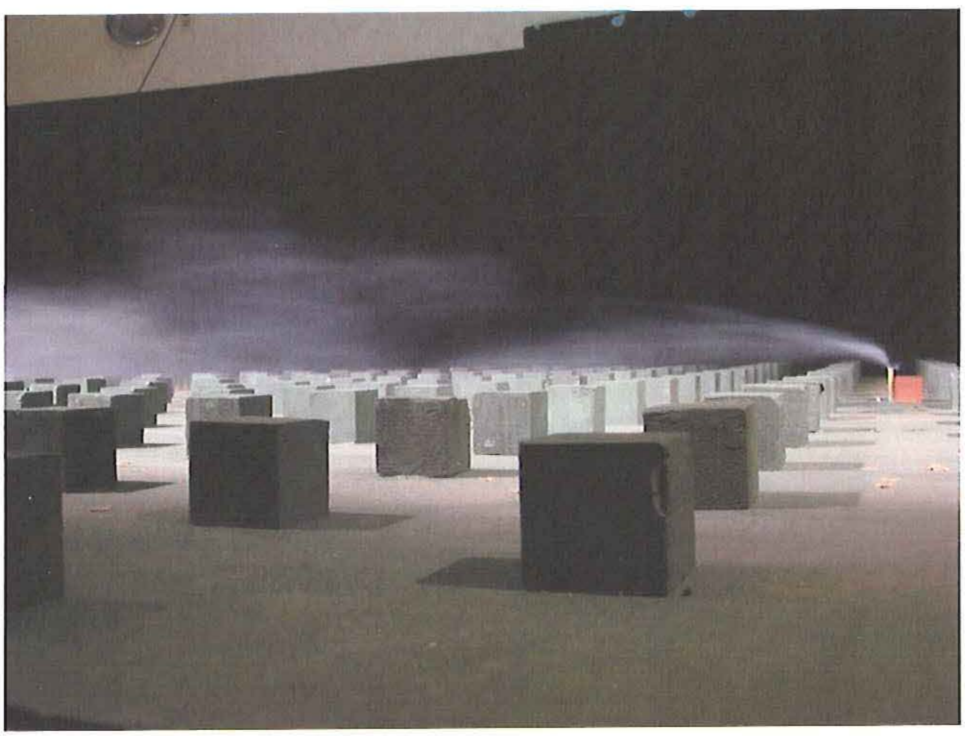

d)

Figure 16. Photographs of selected exhaust plume flow visualizations for stack S_349: c) EBD tests: no building in place; d) EBD tests: EBD 4 (1:2:1) with a full scale height of 16 m in place.

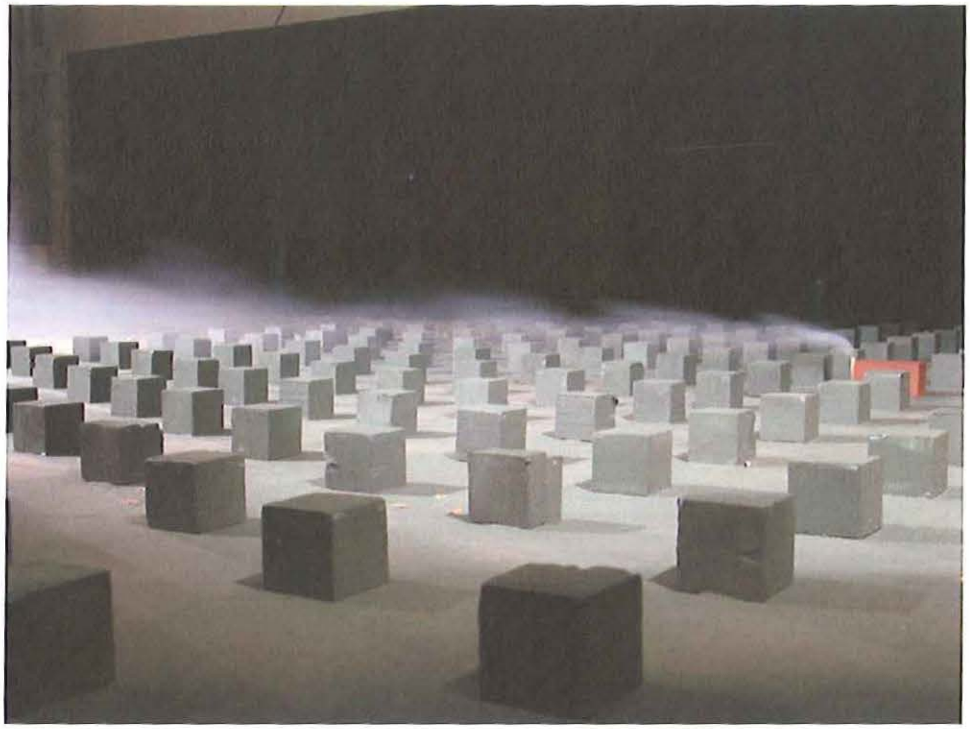

e)

Figure 16. Photographs of selected exhaust plume flow visualizations for stack S_349: e) EBD tests: EBD 5 (1:1:2) with a full scale height of 20 m in place.

**TABLES**

## Table 1
## Full-scale Exhaust and Modeling Information

English Units

| Source Description | Source ID | Initial Source Height Above Base (ft) | Exit Diameter (in) | Exit Temp. (°F) | Mass Flow (lb/hr) | Volume Flow Rate (cfm) | Exit Velocity (f/s) | Ambient Temperature (°F) | Source Base Elevation (ft) | PM10 (lb/hr) |
|---|---|---|---|---|---|---|---|---|---|---|
| 1 Pahts 144 Taper | S_071 | 76.3 | 42.0 | 70.0 | 153,702 | 33,712 | 58.4 | 70.0 | 0.0 | 1.55 |
| 2 100 5 Stand Hot Mill - N | S_288 | 87.2 | 108.0 | 108.0 | 607,291 | 142,757 | 37.4 | 72.7 | 0.0 | 12.92 |
| 3 100 5 Stand Hot Mill - S | S_289 | 87.2 | 108.0 | 100.0 | 615,972 | 142,757 | 37.4 | 72.7 | 0.0 | 12.92 |
| 4 144 Hot Mill | S_344 | 84.6 | 87.6 | 85.0 | 654,675 | 147,660 | 58.8 | 72.7 | 0.0 | 9.46 |
| 5 160 Hot Mill | S_349 | 69.7 | 97.2 | 100.0 | 780,423 | 180,870 | 58.5 | 72.7 | 0.0 | 15.42 |
| 6 Reynolds number stack | Re S_071 | 76.3 | 42.0 | 70.0 | 153,700 | 33,712 | 58.4 | 70.0 | 0.0 | 1.55 |

Metric Units

| Source Description | Source ID | Initial Source Height Above Base (m) | Exit Diameter (m) | Exit Temp. (K) | Mass Flow (kg/s) | Volume Flow Rate ($m^3$/s) | Exit Velocity (m/s) | Ambient Temperature (K) | Source Base Height Above Grade (m) | PM10 (g/s) |
|---|---|---|---|---|---|---|---|---|---|---|
| 1 Pahts 144 Taper | S_071 | 23.3 | 1.07 | 294.3 | 19.41 | 15.91 | 17.80 | 294.3 | 0.0 | 11.74 |
| 2 100 5 Stand Hot Mill - N | S_288 | 26.6 | 2.74 | 315.4 | 76.68 | 67.37 | 11.40 | 295.8 | 0.0 | 97.66 |
| 3 100 5 Stand Hot Mill - S | S_289 | 26.6 | 2.74 | 310.9 | 77.77 | 67.37 | 11.40 | 295.8 | 0.0 | 97.66 |
| 4 144 Hot Mill | S_344 | 25.8 | 2.23 | 302.6 | 82.66 | 69.69 | 17.92 | 295.8 | 0.0 | 71.55 |
| 5 160 Hot Mill | S_349 | 21.3 | 2.47 | 310.9 | 98.54 | 85.36 | 17.83 | 295.8 | 0.0 | 116.58 |
| 6 Reynolds number stack | Re S_071 | 23.3 | 1.07 | 294.3 | 19.41 | 15.91 | 17.80 | 294.3 | 0.0 | 11.74 |

**Site Parameters:**

| | | |
|---|---|---|
| Scale Reduction: | 400 | |
| Grade Elevation (m): | 175.9 | 577 ft msl |
| Typical Building Height (m): | 25.0 | |
| Ambient Temperature (°K): | 295.8 | Moline Surface Met Data 2000-2004 (72.7 F. Average Summer Temperature) |
| Anemometer Height (m): | 10.00 | Moline Surface Met Data 2000-2004 |
| Anemometer Surface Roughness (m): | 0.07 | |
| Site Anemometer Height (m): | 10.00 | |
| Site Surface Roughness (m): | 0.08 | |
| 2 % Wind Speed | 9.0 | (Period of Record: 2000-2004) |

Google Locations:
S_071 712197.24 4601727.73
S_288 712040.15 4601636.08
S_289 712045.26 4601628.32
S_344 712159.72 4601621.72
S_349 712294.69 4601699.52

cpp

**Table 2**
**Surface Roughness Values (Zo) Determined by AERSURFACE and Zo Values Used in Wind Tunnel Simulations**

| AERSURFACE Sectors (Degrees) | 0.732 km Radius AERSURFACE Zo (m) (1) | 3 km Radius AERSURFACE Zo (m) (2) | Wind Tunnel Test Sectors (Degrees) | Wind Tunnel Test Zo (m) (3) |
|---|---|---|---|---|
| 0-30 | 0.771 | 0.382 | NA | NA |
| 30-60 | 0.801 | 0.147 | NA | NA |
| 60-90 | 0.700 | 0.032 | NA | NA |
| 90-120 | 0.278 | 0.036 | 100 to 240 | 0.084 |
| 120-150 | 0.188 | 0.090 | | |
| 150-180 | 0.614 | 0.127 | | |
| 180-210 | 0.785 | 0.065 | | |
| 210-240 | 0.797 | 0.107 | | |
| 240-270 | 0.801 | 0.737 | 250 and 260 | 0.737 |
| 270-300 | 0.669 | 0.454 | NA | NA |
| 300-330 | 0.794 | 0.266 | NA | NA |
| 330-360 | 0.693 | 0.473 | NA | NA |
| Mean | 0.658 | 0.243 | | |

1) Used for the EBD part of the study. Mean Zo defines the appropriate surface roughness length for the turntable.
2) Used to define the appropriate surface roughness length for approach flows in the wind tunnel.
3) Mean Zo values used for the approach flows.

**Table 3**
**Concentration Measurment Test Plan**

| Run No. | Source 1 ID | Stack Height Above Base (ft) | Tracer Gas | Source 2 ID | Stack Height Above Base (ft) | Tracer Gas | Wind Direction (Deg.) | Model Reference Wind Speed (m/s) | 2% Airport Wind Speed (m/s) | Approach Zo (m) |
|---|---|---|---|---|---|---|---|---|---|---|
| **Reynolds Number Independence Tests** | | | | | | | | | | |
| 1 | Re S_071 | 76.3 | Ethane | | | | 140 | 5.50 | 9.00 | 0.084 |
| 2 | Re S_071 | 76.3 | Ethane | | | | 140 | 4.00 | 9.00 | 0.084 |
| 3 | Re S_071 | 76.3 | Ethane | | | | 140 | 3.00 | 9.00 | 0.084 |
| **Tests with Site Structure Present** | | | | | | | | | | |
| 101 | S_071 | 76.3 | Ethane | | | | 100 | 4.00 | 9.00 | 0.084 |
| 102 | S_071 | 76.3 | Ethane | | | | 110 | 4.00 | 9.00 | 0.084 |
| 103 | S_071 | 76.3 | Ethane | | | | 120 | 4.00 | 9.00 | 0.084 |
| 104 | S_071 | 76.3 | Ethane | | | | 130 | 4.00 | 9.00 | 0.084 |
| 105 | S_071 | 76.3 | Ethane | | | | 140 | 4.00 | 9.00 | 0.084 |
| 106 | S_071 | 76.3 | Ethane | | | | 150 | 4.00 | 9.00 | 0.084 |
| 107 | S_071 | 76.3 | Ethane | | | | 160 | 4.00 | 9.00 | 0.084 |
| 108 | S_071 | 76.3 | Ethane | | | | 170 | 4.00 | 9.00 | 0.084 |
| 109 | S_071 | 76.3 | Ethane | | | | 220 | 4.00 | 9.00 | 0.084 |
| 110 | S_071 | 76.3 | Ethane | | | | 230 | 4.00 | 9.00 | 0.084 |
| 111 | S_071 | 76.3 | Ethane | | | | 240 | 4.00 | 9.00 | 0.084 |
| 112 | S_071 | 76.3 | Ethane | | | | 250 | 3.88 | 9.00 | 0.737 |
| 113 | S_071 | 76.3 | Ethane | | | | 260 | 3.88 | 9.00 | 0.737 |
| | | | | | | | | | | |
| 114 | S_288 | 87.2 | Methane | S_289 | 87.2 | Ethane | 100 | 4.00 | 9.00 | 0.084 |
| 115 | S_288 | 87.2 | Methane | S_289 | 87.2 | Ethane | 110 | 4.00 | 9.00 | 0.084 |
| 116 | S_288 | 87.2 | Methane | S_289 | 87.2 | Ethane | 120 | 4.00 | 9.00 | 0.084 |
| 117 | S_288 | 87.2 | Methane | S_289 | 87.2 | Ethane | 130 | 4.00 | 9.00 | 0.084 |
| 118 | S_288 | 87.2 | Methane | S_289 | 87.2 | Ethane | 140 | 4.00 | 9.00 | 0.084 |
| 119 | S_288 | 87.2 | Methane | S_289 | 87.2 | Ethane | 150 | 4.00 | 9.00 | 0.084 |
| 120 | S_288 | 87.2 | Methane | S_289 | 87.2 | Ethane | 160 | 4.00 | 9.00 | 0.084 |
| 121 | S_288 | 87.2 | Methane | S_289 | 87.2 | Ethane | 170 | 4.00 | 9.00 | 0.084 |
| 122 | S_288 | 87.2 | Methane | S_289 | 87.2 | Ethane | 220 | 4.00 | 9.00 | 0.084 |
| 123 | S_288 | 87.2 | Methane | S_289 | 87.2 | Ethane | 230 | 4.00 | 9.00 | 0.084 |
| 124 | S_288 | 87.2 | Methane | S_289 | 87.2 | Ethane | 240 | 4.00 | 9.00 | 0.084 |
| 125 | S_288 | 87.2 | Methane | S_289 | 87.2 | Ethane | 250 | 3.88 | 9.00 | 0.737 |
| 126 | S_288 | 87.2 | Methane | S_289 | 87.2 | Ethane | 260 | 3.88 | 9.00 | 0.737 |
| | | | | | | | | | | |
| 127 | S_344 | 84.6 | Methane | S_349 | 69.7 | Ethane | 100 | 4.00 | 9.00 | 0.084 |
| 128 | S_344 | 84.6 | Methane | S_349 | 69.7 | Ethane | 110 | 4.00 | 9.00 | 0.084 |
| 129 | S_344 | 84.6 | Methane | S_349 | 69.7 | Ethane | 120 | 4.00 | 9.00 | 0.084 |
| 130 | S_344 | 84.6 | Methane | S_349 | 69.7 | Ethane | 130 | 4.00 | 9.00 | 0.084 |
| 131 | S_344 | 84.6 | Methane | S_349 | 69.7 | Ethane | 140 | 4.00 | 9.00 | 0.084 |
| 132 | S_344 | 84.6 | Methane | S_349 | 69.7 | Ethane | 150 | 4.00 | 9.00 | 0.084 |
| 133 | S_344 | 84.6 | Methane | S_349 | 69.7 | Ethane | 160 | 4.00 | 9.00 | 0.084 |
| 134 | S_344 | 84.6 | Methane | S_349 | 69.7 | Ethane | 170 | 4.00 | 9.00 | 0.084 |
| 135 | S_344 | 84.6 | Methane | S_349 | 69.7 | Ethane | 220 | 4.00 | 9.00 | 0.084 |
| 136 | S_344 | 84.6 | Methane | S_349 | 69.7 | Ethane | 230 | 4.00 | 9.00 | 0.084 |
| 137 | S_344 | 84.6 | Methane | S_349 | 69.7 | Ethane | 240 | 4.00 | 9.00 | 0.084 |
| 138 | S_344 | 84.6 | Methane | S_349 | 69.7 | Ethane | 250 | 3.88 | 9.00 | 0.737 |
| 139 | S_344 | 84.6 | Methane | S_349 | 69.7 | Ethane | 260 | 3.88 | 9.00 | 0.737 |
| | | | | | | | | | | |
| 140 | S_071 | 76.3 | Ethane | | | | 180 | 4.00 | 9.00 | 0.084 |
| 141 | S_071 | 76.3 | Ethane | | | | 190 | 4.00 | 9.00 | 0.084 |
| 142 | S_071 | 76.3 | Ethane | | | | 200 | 4.00 | 9.00 | 0.084 |
| 143 | S_071 | 76.3 | Ethane | | | | 210 | 4.00 | 9.00 | 0.084 |
| | | | | | | | | | | |
| 144 | S_288 | 87.2 | Methane | S_289 | 87.2 | Ethane | 180 | 4.00 | 9.00 | 0.084 |
| 145 | S_288 | 87.2 | Methane | S_289 | 87.2 | Ethane | 190 | 4.00 | 9.00 | 0.084 |
| 146 | S_288 | 87.2 | Methane | S_289 | 87.2 | Ethane | 200 | 4.00 | 9.00 | 0.084 |
| 147 | S_288 | 87.2 | Methane | S_289 | 87.2 | Ethane | 210 | 4.00 | 9.00 | 0.084 |
| | | | | | | | | | | |
| 148 | S_344 | 84.6 | Methane | S_349 | 69.7 | Ethane | 180 | 4.00 | 9.00 | 0.084 |
| 149 | S_344 | 84.6 | Methane | S_349 | 69.7 | Ethane | 190 | 4.00 | 9.00 | 0.084 |
| 150 | S_344 | 84.6 | Methane | S_349 | 69.7 | Ethane | 200 | 4.00 | 9.00 | 0.084 |
| 151 | S_344 | 84.6 | Methane | S_349 | 69.7 | Ethane | 210 | 4.00 | 9.00 | 0.084 |

**Table 3 (continued)**
**Concentration Measurment Test Plan**

| Run No. | Source 1 ID | Stack Height Above Base (ft) | Tracer Gas | EBD ID Model Scale (cm) | EBD Height Full Scale (m) | EBD Aspect Ratio Hb : | W : | L | EBD Comments | Model Reference Wind Speed (m/s) | 2% Airport Wind Speed (m/s) | Approach Zo (m) |
|---|---|---|---|---|---|---|---|---|---|---|---|---|
| **EBD Tests** | | | | | | | | | | | | |
| 201 | S_071 | 76.3 | Ethane | no EBD | 0 | | | | | 4.00 | 9.00 | 0.084 |
| 202 | S_071 | 76.3 | Ethane | EBD 3 | 12 | 1 | 2 | 1 | | 4.00 | 9.00 | 0.084 |
| 203 | S_071 | 76.3 | Ethane | EBD 4 | 16 | 1 | 2 | 1 | | 4.00 | 9.00 | 0.084 |
| 204 | S_071 | 76.3 | Ethane | EBD 5 | 20 | 1 | 2 | 1 | | 4.00 | 9.00 | 0.084 |
| 205 | S_071 | 76.3 | Ethane | EBD 5.5 | 22 | 1 | 2 | 1 | | 4.00 | 9.00 | 0.084 |
| 206 | S_071 | 76.3 | Ethane | EBD 5 | 20 | 1 | 4 | 1 | | 4.00 | 9.00 | 0.084 |
| 207 | S_071 | 76.3 | Ethane | EBD 5 | 20 | 1 | 6 | 1 | | 4.00 | 9.00 | 0.084 |
| 208 | S_071 | 76.3 | Ethane | EBD 5 | 20 | 1 | 2 | 2 | rotated 45 degrees | 4.00 | 9.00 | 0.084 |
| 209 | S_071 | 76.3 | Ethane | EBD 5 | 20 | 1 | 1 | 1 | | 4.00 | 9.00 | 0.084 |
| 210 | S_071 | 76.3 | Ethane | EBD 5 | 20 | 1 | 2 | 1 | downwind of stack | 4.00 | 9.00 | 0.084 |
| 211 | S_071 | 76.3 | Ethane | no EBD | 0 | | | | | 3.88 | 9.00 | 0.737 |
| | | | | | | | | | | | | |
| 221 | S_288 | 87.2 | Methane | no EB | 0 | | | | | 4.00 | 9.00 | 0.084 |
| 222 | S_288 | 87.2 | Methane | EBD 6 | 24 | 1 | 4 | 1 | | 4.00 | 9.00 | 0.084 |
| | | | | | | | | | | | | |
| 241 | S_289 | 87.2 | Ethane | no EB | 0 | | | | | 4.00 | 9.00 | 0.084 |
| 242 | S_289 | 87.2 | Ethane | EBD 3 | 12 | 1 | 2 | 1 | | 4.00 | 9.00 | 0.084 |
| 243 | S_289 | 87.2 | Ethane | EBD 4 | 16 | 1 | 2 | 1 | | 4.00 | 9.00 | 0.084 |
| 244 | S_289 | 87.2 | Ethane | EBD 5 | 20 | 1 | 2 | 1 | | 4.00 | 9.00 | 0.084 |
| 245 | S_289 | 87.2 | Ethane | EBD 6 | 24 | 1 | 4 | 1 | | 4.00 | 9.00 | 0.084 |
| 246 | S_289 | 87.2 | Ethane | no EB | 0 | | | | | 3.88 | 9.00 | 0.737 |
| | | | | | | | | | | | | |
| 261 | S_344 | 84.6 | Methane | no EB | 0 | | | | | 4.00 | 9.00 | 0.084 |
| 262 | S_344 | 84.6 | Methane | EBD 3 | 12 | 1 | 2 | 1 | | 4.00 | 9.00 | 0.084 |
| 263 | S_344 | 84.6 | Methane | EBD 4 | 16 | 1 | 2 | 1 | | 4.00 | 9.00 | 0.084 |
| 264 | S_344 | 84.6 | Methane | EBD 5 | 20 | 1 | 2 | 1 | | 4.00 | 9.00 | 0.084 |
| 265 | S_344 | 84.6 | Methane | no EB | 0 | | | | | 3.88 | 9.00 | 0.737 |
| | | | | | | | | | | | | |
| 281 | S_349 | 69.7 | Ethane | no EB | 0 | | | | | 4.00 | 9.00 | 0.084 |
| 282 | S_349 | 69.7 | Ethane | EBD 5.5 | 22 | 1 | 2 | 1 | | 4.00 | 9.00 | 0.084 |
| 283 | S_349 | 69.7 | Ethane | EBD 4.5 | 18 | 1 | 2 | 1 | | 4.00 | 9.00 | 0.084 |
| 284 | S_349 | 69.7 | Ethane | EBD 3 | 12 | 1 | 2 | 1 | | 4.00 | 9.00 | 0.084 |
| 285 | S_349 | 69.7 | Ethane | EBD 4 | 16 | 1 | 2 | 1 | | 4.00 | 9.00 | 0.084 |
| 286 | S_349 | 69.7 | Ethane | EBD 4.5 | 18 | 1 | 4 | 1 | | 4.00 | 9.00 | 0.084 |
| 287 | S_349 | 69.7 | Ethane | EBD 5 | 20 | 1 | 4 | 1 | | 4.00 | 9.00 | 0.084 |
| 288 | S_349 | 69.7 | Ethane | EBD 4.5 | 18 | 1 | 2 | 3 | | 4.00 | 9.00 | 0.084 |
| 289 | S_349 | 69.7 | Ethane | EBD 4.5 | 18 | 1 | 2 | 2 | rotated 45 degrees | 4.00 | 9.00 | 0.084 |
| 290 | S_349 | 69.7 | Ethane | EBD 5 | 20 | 1 | 1 | 2 | | 4.00 | 9.00 | 0.084 |
| 291 | S_349 | 69.7 | Ethane | no EB | 0 | | | | | 3.88 | 9.00 | 0.737 |
| | | | | | | | | | | | | |
| 302 | S_071 | 76.3 | Ethane | EBD 6 | 24 | 1 | 2 | 1 | | 4.00 | 9.00 | 0.084 |
| 303 | S_071 | 76.3 | Ethane | EBD 5.5 | 22 | 1 | 2 | 1 | rotated 63 degrees | 4.00 | 9.00 | 0.084 |
| 304 | S_071 | 76.3 | Ethane | EBD 6 | 24 | 1 | 2 | 1 | rotated 63 degrees | 4.00 | 9.00 | 0.084 |
| 305 | S_071 | 76.3 | Ethane | EBD 5 | 20 | 1 | 2 | 1 | rotated 63 degrees | 4.00 | 9.00 | 0.084 |
| 306 | S_071 | 76.3 | Ethane | EBD 5.5 | 22 | 1 | 4 | 1 | rotated 63 degrees | 4.00 | 9.00 | 0.084 |
| 307 | S_071 | 76.3 | Ethane | EBD 5.5 | 22 | 1 | 1 | 1 | rotated 45 degrees | 4.00 | 9.00 | 0.084 |
| 308 | S_071 | 76.3 | Ethane | EBD 5.5 | 22 | 1 | 2 | 1 | rotated 63 degrees | 4.00 | 9.00 | 0.084 |
| | | | | | | | | | | | | |
| 311 | S_289 | 87.2 | Ethane | EBD 4 | 16 | 1 | 2 | 1 | rotated 63 degrees | 4.00 | 9.00 | 0.084 |
| 312 | S_289 | 87.2 | Ethane | EBD 5 | 20 | 1 | 2 | 1 | rotated 63 degrees | 4.00 | 9.00 | 0.084 |
| | | | | | | | | | | | | |
| 321 | S_344 | 84.6 | Methane | EBD 5.5 | 22 | 1 | 2 | 1 | | 4.00 | 9.00 | 0.084 |

**Table 4a**
**Equivalent Building Dimensions for Input into AERMOD**
**Alcoa Davenport Works**
**Stack: S_071**

| Flow Vector (Deg.) | Wind Direction (Deg.) | EBD ID | BUILDHGT Hb (m) | BUILDWID W (m) | BUILDLEN L (m) | XBADJ (m) | YBADJ (m) | Aspect Ratio Hb: | W: | L |
|---|---|---|---|---|---|---|---|---|---|---|
| 280 | 100 | 4 | 16 | 32 | 16 | -16 | 0 | 1 | 2 | 1 |
| 290 | 110 | 5 | 20 | 56.6 | 56.6 | -56.6 | 0 | 1 | 2.8 | 2.8 |
| 300 | 120 | 5 | 20 | 56.6 | 56.6 | -56.6 | 0 | 1 | 2.8 | 2.8 |
| 310 | 130 | 5 | 20 | 20 | 20 | -20 | 0 | 1 | 1 | 1 |
| 320 | 140 | 0 | 0 | 0 | 0 | 0 | 0 | | | |
| 330 | 150 | 3 | 12 | 24 | 12 | -12 | 0 | 1 | 2 | 1 |
| 340 | 160 | 5 | 20 | 20 | 20 | -20 | 0 | 1 | 1 | 1 |
| 350 | 170 | 3 | 12 | 24 | 12 | -12 | 0 | 1 | 2 | 1 |
| 360 | 180 | 4 | 16 | 32 | 16 | -16 | 0 | 1 | 2 | 1 |
| 10 | 190 | 5.5 | 22 | 39.6 | 48.4 | -48.4 | 0 | 1 | 1.8 | 2.2 |
| 20 | 200 | 5.5 | 22 | 39.6 | 48.4 | -48.4 | 0 | 1 | 1.8 | 2.2 |
| 30 | 210 | 5 | 20 | 36 | 44 | -44 | 0 | 1 | 1.8 | 2.2 |
| 40 | 220 | 5 | 20 | 56.6 | 56.6 | -56.6 | 0 | 1 | 2.8 | 2.8 |
| 50 | 230 | 3 | 12 | 24 | 12 | -12 | 0 | 1 | 2 | 1 |
| 60 | 240 | 0 | 0 | 0 | 0 | 0 | 0 | | | |
| 70 | 250 | 0 | 0 | 0 | 0 | 0 | 0 | | | |
| 80 | 260 | 0 | 0 | 0 | 0 | 0 | 0 | | | |

**Table 4b**
**Equivalent Building Dimensions for Input into AERMOD**
**Alcoa Davenport Works**
**Stack: S_288**

| Flow Vector (Deg.) | Wind Direction (Deg.) | EBD ID | BUILDHGT Hb (m) | BUILDWID W (m) | BUILDLEN L (m) | XBADJ (m) | YBADJ (m) | Aspect Ratio Hb: | W: | L |
|---|---|---|---|---|---|---|---|---|---|---|
| 280 | 100 | 3 | 12 | 24 | 12 | -12 | 0 | 1 | 2 | 1 |
| 290 | 110 | 0 | 0 | 0 | 0 | 0 | 0 | | | |
| 300 | 120 | 0 | 0 | 0 | 0 | 0 | 0 | | | |
| 310 | 130 | 0 | 0 | 0 | 0 | 0 | 0 | | | |
| 320 | 140 | 0 | 0 | 0 | 0 | 0 | 0 | | | |
| 330 | 150 | 3 | 12 | 24 | 12 | -12 | 0 | 1 | 2 | 1 |
| 340 | 160 | 0 | 0 | 0 | 0 | 0 | 0 | | | |
| 350 | 170 | 0 | 0 | 0 | 0 | 0 | 0 | | | |
| 360 | 180 | 3 | 12 | 24 | 12 | -12 | 0 | 1 | 2 | 1 |
| 10 | 190 | 4 | 16 | 32 | 16 | -16 | 0 | 1 | 2 | 1 |
| 20 | 200 | 5 | 20 | 40 | 20 | -20 | 0 | 1 | 2 | 1 |
| 30 | 210 | 0 | 0 | 0 | 0 | 0 | 0 | | | |
| 40 | 220 | 0 | 0 | 0 | 0 | 0 | 0 | | | |
| 50 | 230 | 4 | 16 | 32 | 16 | -16 | 0 | 1 | 2 | 1 |
| 60 | 240 | 0 | 0 | 0 | 0 | 0 | 0 | | | |
| 70 | 250 | 0 | 0 | 0 | 0 | 0 | 0 | | | |
| 80 | 260 | 0 | 0 | 0 | 0 | 0 | 0 | | | |

**Table 4c**
**Equivalent Building Dimensions for Input into AERMOD**
**Alcoa Davenport Works**
**Stack: S_289**

| Flow Vector (Deg.) | Wind Direction (Deg.) | EBD ID | BUILDHGT Hb (m) GEP | BUILDWID W (m) | BUILDLEN L (m) | XBADJ (m) | YBADJ (m) | Aspect Ratio Hb: | W: | L |
|---|---|---|---|---|---|---|---|---|---|---|
| 280 | 100 | 5 | 20 50 | 40 | 20 | -20 | 0 | 1 | 2 | 1 |
| 290 | 110 | 0 | 0 | 0 | 0 | 0 | 0 | | | |
| 300 | 120 | 3 | 12 30 | 24 | 12 | -12 | 0 | 1 | 2 | 1 |
| 310 | 130 | 0 | 0 | 0 | 0 | 0 | 0 | | | |
| 320 | 140 | 3 | 12 | 24 | 12 | -12 | 0 | 1 | 2 | 1 |
| 330 | 150 | 3 | 12 | 24 | 12 | -12 | 0 | 1 | 2 | 1 |
| 340 | 160 | 0 | 0 | 0 | 0 | 0 | 0 | | | |
| 350 | 170 | 0 | 0 | 0 | 0 | 0 | 0 | | | |
| 360 | 180 | 3 | 12 | 24 | 12 | -12 | 0 | 1 | 2 | 1 |
| 10 | 190 | 3 | 12 | 24 | 12 | -12 | 0 | 1 | 2 | 1 |
| 20 | 200 | 5 | 20 | 40 | 20 | -20 | 0 | 1 | 2 | 1 |
| 30 | 210 | 0 | 0 | 0 | 0 | 0 | 0 | | | |
| 40 | 220 | 0 | 0 | 0 | 0 | 0 | 0 | | | |
| 50 | 230 | 0 | 0 | 0 | 0 | 0 | 0 | | | |
| 60 | 240 | 0 | 0 | 0 | 0 | 0 | 0 | | | |
| 70 | 250 | 0 | 0 | 0 | 0 | 0 | 0 | | | |
| 80 | 260 | 0 | 0 | 0 | 0 | 0 | 0 | | | |

**Table 4d**
**Equivalent Building Dimensions for Input into AERMOD**
**Alcoa Davenport Works**
**Stack: S_344**

| Flow Vector (Deg.) | Wind Direction (Deg.) | EBD ID | BUILDHGT Hb (m) GEP | BUILDWID W (m) | BUILDLEN L (m) | XBADJ (m) | YBADJ (m) | Aspect Ratio Hb: | W: | L |
|---|---|---|---|---|---|---|---|---|---|---|
| 280 | 100 | 0 | 0 | 0 | 0 | 0 | 0 | | | |
| 290 | 110 | 0 | 0 | 0 | 0 | 0 | 0 | | | |
| 300 | 120 | 0 | 0 | 0 | 0 | 0 | 0 | | | |
| 310 | 130 | 0 | 0 | 0 | 0 | 0 | 0 | | | |
| 320 | 140 | 0 | 0 | 0 | 0 | 0 | 0 | | | |
| 330 | 150 | 0 | 0 | 0 | 0 | 0 | 0 | | | |
| 340 | 160 | 0 | 0 | 0 | 0 | 0 | 0 | | | |
| 350 | 170 | 0 | 0 | 0 | 0 | 0 | 0 | | | |
| 360 | 180 | 0 | 0 | 0 | 0 | 0 | 0 | | | |
| 10 | 190 | 4 | 16 40 | 32 | 16 | -16 | 0 | 1 | 2 | 1 |
| 20 | 200 | 5.5 | 22 55 | 44 | 22 | -22 | 0 | 1 | 2 | 1 |
| 30 | 210 | 5 | 20 50 | 40 | 20 | -20 | 0 | 1 | 2 | 1 |
| 40 | 220 | 3 | 12 30 | 24 | 12 | -12 | 0 | 1 | 2 | 1 |
| 50 | 230 | 0 | 0 | 0 | 0 | 0 | 0 | | | |
| 60 | 240 | 0 | 0 | 0 | 0 | 0 | 0 | | | |
| 70 | 250 | 0 | 0 | 0 | 0 | 0 | 0 | | | |
| 80 | 260 | 0 | 0 | 0 | 0 | 0 | 0 | | | |

cpp

**Table 4e**
**Equivalent Building Dimensions for Input into AERMOD**
**Alcoa Davenport Works**
**Stack: S_349**

| Flow Vector (Deg.) | Wind Direction (Deg.) | EBD ID | BUILDHGT Hb (m) GEP | BUILDWID W (m) | BUILDLEN L (m) | XBADJ (m) | YBADJ (m) | Aspect Ratio Hb: | W: | L |
|---|---|---|---|---|---|---|---|---|---|---|
| 280 | 100 | 4.5 | 18 45 | 50.9 | 50.9 | -50.9 | 0 | 1 | 2.8 | 2.8 |
| 290 | 110 | 4.5 | 18 | 50.9 | 50.9 | -50.9 | 0 | 1 | 2.8 | 2.8 |
| 300 | 120 | 5 | 20 50 | 20 | 40 | -40 | 0 | 1 | 1 | 2 |
| 310 | 130 | 5 | 20 | 20 | 40 | -40 | 0 | 1 | 1 | 2 |
| 320 | 140 | 4 | 16 40 | 32 | 16 | -16 | 0 | 1 | 2 | 1 |
| 330 | 150 | 5 | 20 | 20 | 40 | -40 | 0 | 1 | 1 | 2 |
| 340 | 160 | 5 | 20 | 20 | 40 | -40 | 0 | 1 | 1 | 2 |
| 350 | 170 | 4 | 16 | 32 | 16 | -16 | 0 | 1 | 2 | 1 |
| 360 | 180 | 5 | 20 | 20 | 40 | -40 | 0 | 1 | 1 | 2 |
| 10 | 190 | 5 | 20 | 20 | 40 | -40 | 0 | 1 | 1 | 2 |
| 20 | 200 | 0 | 0 | 0 | 0 | 0 | 0 | | | |
| 30 | 210 | 5 | 20 | 20 | 40 | -40 | 0 | 1 | 1 | 2 |
| 40 | 220 | 0 | 0 | 0 | 0 | 0 | 0 | | | |
| 50 | 230 | 0 | 0 | 0 | 0 | 0 | 0 | | | |
| 60 | 240 | 3 | 12 30 | 24 | 12 | -12 | 0 | 1 | 2 | 1 |
| 70 | 250 | 0 | 0 | 0 | 0 | 0 | 0 | | | |
| 80 | 260 | 4 | 16 | 32 | 16 | -16 | 0 | 1 | 2 | 1 |